



U.S. Department  
of Transportation  
**Federal Highway  
Administration**

# **SERVICEABILITY LIMITS AND ECONOMICAL STEEL BRIDGE DESIGN**

---

---

**Publication No. FHWA-HIF-11-044**

**August 2011**

---

**Technical Report Documentation Page**

1. Report No. FHWA-HIF-11-044		2. Government Accession No.		3. Recipient's Catalog No.	
4. Title and Subtitle  <b>SERVICEABILITY LIMITS AND ECONOMICAL STEEL BRIDGE DESIGN</b>			5. Report Date August 2011		
			6. Performing Organization Code		
7. Author(s) Michael G. Barker and James Staebler, University of Wyoming Karl E. Barth, West Virginia University			8. Performing Organization Report No.		
9. Performing Organization Name and Address West Virginia University University of Wyoming			10. Work Unit No. (TRAI5)		
			11. Contract or Grant No.		
12. Sponsoring Agency Name and Address FHWA Office of Bridge Technology 1200 New Jersey Ave SE Washington DC 20590			13. Type of Report and Period Covered Final Report		
			14. Sponsoring Agency Code		
15. Supplementary Notes					
16. Abstract Current AASHTO LRFD Bridge Design Specifications Service I deflection limits are in place with the purpose to prevent deformation-induced structural damage and psychological user-discomfort from excess bridge vibration. Previous research has shown that deflection criterion alone is insufficient in controlling excess bridge vibrations and structural deterioration of the concrete deck. Previous research shows that natural frequency criteria better controls excess vibration than deflection criteria. In addition, previous research shows no significant correlation between deflection and structural deformation of the concrete deck slab. In order to better control excess bridge vibrations and deformation-induced structural deterioration, two new separate criteria formulations are proposed. The first formulation consists of a natural frequency criteria transformed into deflection type terms familiar to the typical bridge engineer. The second proposed formulation directly controls the acting flexural strain in the concrete deck to control deformation-induced structural damage. The proposed serviceability criteria are applied to a database of 195 steel girder bridges. Both the as-built behavior and the design optimized behavior are examined and compared to current AASHTO serviceability criteria.					
17. Key Words			18. Distribution Statement		
19. Security Classif. (of this report) Unclassified		20. Security Classif. (of this page) Unclassified		21. No. of Pages	22. Price

## **PREFACE**

Although the live load deflection criteria found in AASHTO LRFD are given as optional, many owners continue to apply these requirements for the design of new steel bridges. This report proposes two new serviceability criteria for more rational control of bridge vibrations and deformation-induced structural deterioration. The first is a deflection limit that is related to the estimated natural frequency of the bridge to maintain user comfort and the second is a limit on the flexural strain in the concrete deck to control deformation-induced structural damage. The proposed criteria have been applied to a database of 195 steel girder bridges. Both the as-built behavior and the design optimized behavior are examined and compared to the current AASHTO LRFD serviceability criteria. Future calibration work may be necessary to establish an appropriate threshold and safety index for these limit states prior to adoption by AASHTO.

## **NOTICE**

The Federal Highway Administration provides high-quality information to serve Government, industry, and the public in a manner that promotes public understanding. Standards and policies are used to ensure and maximize the quality, objectivity, utility, and integrity of its information. FHWA periodically reviews quality issues and adjusts its programs and processes to ensure continuous quality improvement.

# Table of Contents

<b>CHAPTER 1 INTRODUCTION.....</b>	<b>1</b>
1.1 Background.....	1
1.2 Objectives .....	3
1.3 Organization.....	5
<b>CHAPTER 2 BACKGROUND.....</b>	<b>7</b>
2.1 Introduction and Live Load Deflection Criteria.....	7
2.2 Live Load Deflection Studies .....	8
2.3 Bridge Summary.....	11
2.4 Summary .....	13
<b>CHAPTER 3 USER COMFORT CRITERIA .....</b>	<b>14</b>
3.1 Introduction .....	14
3.2 Derivation of User Comfort Formulation.....	14
3.2.1 Dynamic Pluck Test.....	14
3.2.2 Correlating $X_{lim}$ to the OHBC Criteria.....	21
3.2.2.1 OHBC Criteria.....	21
3.2.2.2 Correlating $X_{lim}$ to OHBC Criteria .....	25
3.3 Sample Calculations Using Missouri Bridge A6101 .....	28
3.3.1 Calculating Bridge Properties .....	28
3.3.1.1 Calculating the Distributed Weight (w).....	28
3.3.1.2 Midspan Moment of Inertia.....	32
3.3.1.3 Calculating $c_n$ .....	33
3.3.2 Sample Calculations for Deflections.....	34
3.3.3 Sample Natural Frequency Calculations.....	36
3.3.4 Sample X Factor Calculations.....	37
3.4 Results for Bridges with As-Built Loading.....	37
3.4.1 Service I Deflections.....	37
3.4.2 Fatigue Deflections .....	39
3.4.3 $X_{fat}$ As-Built .....	44
3.4.4 Allowable Deflections.....	46
3.5 Bridge Optimization .....	53

3.5.1	Derivation of Bridge Optimization .....	54
3.5.1.1	Strength I .....	54
3.5.1.2	Service II .....	55
3.5.1.3	Service I .....	56
3.5.1.4	Optimized Rating Factor .....	58
3.5.2	Calculating Optimized Deflections and X factors.....	59
3.5.2.1	Derivation.....	59
3.5.2.2	Sample Calculations for Missouri Bridge A6101 .....	62
3.5.2.2.1	Calculating Optimized Deflections.....	62
3.5.2.2.2	Calculating Optimized X Factors .....	62
3.5.3	Results for Bridges with Optimized Loading.....	63
3.5.3.1	Optimized Service I Deflections.....	63
3.5.3.2	Optimized Fatigue Deflections.....	65
3.5.3.3	Optimized Fatigue X factors and $X_{lim}$ .....	70
3.5.3.4	Optimized Deflection Ratios .....	72
<b>3.6</b>	<b>Summary .....</b>	<b>74</b>
 <b>CHAPTER 4 STRESS AND STRAIN IN THE CONCRETE SLAB .....</b>		<b>76</b>
<b>4.1</b>	<b>Introduction .....</b>	<b>76</b>
<b>4.2</b>	<b>Method for Calculating Stress and Strain in the Concrete Deck.....</b>	<b>77</b>
<b>4.3</b>	<b>Application of Procedure to BridgeTech Database Bridges.....</b>	<b>79</b>
<b>4.4</b>	<b>Alternative Proposed Limit.....</b>	<b>82</b>
<b>4.5</b>	<b>Summary .....</b>	<b>83</b>
 <b>CHAPTER 5 SUMMARY, CONCLUSIONS AND FUTURE WORK .....</b>		<b>84</b>
<b>5.1</b>	<b>Summary .....</b>	<b>84</b>
<b>5.2</b>	<b>Conclusions.....</b>	<b>85</b>
5.2.1	AASHTO Service I Deflection Limit Conclusions.....	86
5.2.2	Alternative Proposed User Comfort Limit Based on $X_{lim}$ Conclusions .....	87
5.2.3	Alternative Proposed Concrete Strain Limit Conclusions.....	88
<b>5.3</b>	<b>Future Work .....</b>	<b>89</b>
5.3.1	Future Work for $X_{lim}$ User Comfort Method.....	89
5.3.2	Future Work for Strain Limit .....	90

## Table of Figures

Figure 2-1 Exterior vs. Interior Girder Behavior Simple Span.....	13
Figure 3-1 Ontario Bridge Code Natural Frequency vs. Maximum Allowable Deflection (OHBC 1983).....	22
Figure 3-2 Approximate & Actual Deflection vs. 1st Natural Frequency....	24
Figure 3-3 Approximate & Actual Deflection vs. 1st Natural Frequency Log-Log Axis.....	24
Figure 3-4 Service I Deflections vs. Span Length Simple Spans .....	38
Figure 3-5 Service I Deflections vs. Span Length Continuous Spans .....	38
Figure 3-6 Fatigue Deflections vs. Span Length Simple Spans.....	40
Figure 3-7 Fatigue Deflections vs. Span Length Continuous Spans .....	40
Figure 3-8 Fatigue As-Built Deflections vs. Natural Frequencies for Simple Spans .....	41
Figure 3-9 Fatigue As-Built Deflections vs. Natural Frequencies for Simple Spans Log-Log Axis .....	42
Figure 3-10 Fatigue As-Built Deflections vs. Natural Frequencies for Continuous Spans.....	42
Figure 3-11 Fatigue As-Built Deflections vs. Natural Frequencies for Continuous Spans Log-Log Axis.....	43
Figure 3-12 $X_{fat\ As-Built}$ , $X_{lim}$ , vs. Span Length Simple Spans.....	45
Figure 3-13 $X_{fat\ As-Built}$ , $X_{lim}$ , vs. Span Length Continuous Spans.....	45
Figure 3-14 $\Delta_{fatAs-Built}/\Delta_{Allowable}$ vs. Span Length Simple Spans.....	47
Figure 3-15 $\Delta_{fatAs-Built}/\Delta_{Allowable}$ vs. Span Length Continuous Spans .....	47
Figure 3-16 Maximum Allowable Deflections No Intended Pedestrian Use Simple Spans.....	49
Figure 3-17 Maximum Allowable Deflections No Intended Pedestrian Use Continuous Spans.....	49
Figure 3-18 Maximum Allowable Deflections Some Intended Pedestrian Use Simple Spans.....	50
Figure 3-19 Maximum Allowable Deflections Some Intended Pedestrian Use Continuous Spans.....	50
Figure 3-20 Maximum Allowable Deflections Heavy Intended Pedestrian Use Simple Spans .....	51
Figure 3-21 Maximum Allowable Deflections Heavy Intended Pedestrian Use Continuous Spans .....	51
Figure 3-22 Optimized Service I Deflections vs. Span Length Simple Spans .....	64
Figure 3-23 Optimized Service I Deflection vs. Span Length Continuous Spans .....	65
Figure 3-24 Optimized Fatigue Deflections vs. Span Length Simple Spans	66

Figure 3-25 Optimized Fatigue Deflections vs. Span Length Continuous Spans.....	67
Figure 3-26 Optimized Fatigue Deflections vs. Natural Frequency for Simple Spans.....	68
Figure 3-27 Optimized Fatigue Deflections vs. Natural Frequency for Simple Spans Log-Log Axis.....	68
Figure 3-28 Optimized Fatigue Deflections vs. Natural Frequency for Continuous Spans.....	69
Figure 3-29 Optimized Fatigue Deflections vs. Natural Frequency for Continuous Spans Log-Log Axis.....	69
Figure 3-30 $X_{fat\ Optimized}$ , $X_{lim}$ , vs. Span Length Simple Spans.....	71
Figure 3-31 $X_{fat\ Optimized}$ , $X_{lim}$ , vs. Span Length Continuous Spans.....	71
Figure 3-32 $\Delta_{fatOptimized}/\Delta_{Allowable}$ vs. Span Length Simple Spans.....	73
Figure 3-33 $\Delta_{fatOptimized}/\Delta_{Allowable}$ vs. Span Length Continuous Spans.....	73
Figure 4-1 Tensile Stress in Concrete Deck vs. Span Length.....	80
Figure 4-2 Tensile Strain in Concrete Deck vs. Span Length.....	80
Figure 4-3 Tensile Stress in Concrete Deck vs. Service I Deflection.....	81
Figure 4-4 Tensile Strain in Concrete Deck vs. Service I Deflection.....	81



## Table of Tables

Table 2-1 Bridge Database Property Summary .....	12
Table 3-1 $\lambda^2$ Coefficients .....	17
Table 3-2 $X_{lim}$ for Various Levels of Anticipated Pedestrian Use.....	27
Table 3-3 Steel Section Distributed Weight Properties .....	29
Table 3-4 Concrete Haunch Distributed Weight Properties .....	30

# **Chapter 1 Introduction**

## **1.1 Background**

The American Association of State Highway and Transportation Officials (AASHTO) LRFD 2002 Bridge Design Specifications contain serviceability deflection criteria perceived to control excess bridge vibrations and structural deterioration. Results of past research efforts indicate that the current AASHTO serviceability deflection criteria is inadequate in controlling excess bridge vibration and structural deterioration. These past studies also state that bridge vibration is better controlled by a limit based on a dynamic property of the bridge, such as natural frequency (Barth, Bergman, Roeder, 2002).

The accelerations associated with excess bridge vibrations are known to cause violations to the bridge user's comfort. Humans have two classifications of response to accelerations associated with bridge vibrations. One response classification type is physiological. This is a physical response that occurs when the bridge vibrates at a frequency that approaches resonance with the natural frequency of the internal organs of the human body. This can cause physical discomfort to the bridge users. The second response classification type is psychological. This is a mental response resulting from unexpected motion. The activity a person is performing

affects the acceptable level of acceleration the person is able to tolerate. A common example is comparing a person working in an office to a person walking on a bridge of a busy street. The person in the office is in a quiet environment not anticipating sudden accelerations and, therefore, the person is more susceptible to acceleration than when in a noisy environment and anticipating sudden accelerations, such as a bridge with heavy traffic (Allen, Murray, & Ungar 1997).

The most common form of structural deterioration for a steel girder, whether composite or not, is cracking in the concrete deck slab. There are many causes for deck cracking including: plastic shrinkage, deck restraint, drying shrinkage, long term flexure under service loads, and repetitive bridge vibrations (Fountain and Thunman 1987).

AASHTO applies deflection serviceability limits that are perceived to limit user discomfort and deck deterioration from flexure. For lower strength steel, the deflection limits have not encroached on bridge economics. With the introduction of high performance steel (HPS) in bridge design, the deflection limit has become more critical in design. HPS designs require less steel that result in larger deflections and, thus deflection limits can impact the economy of a bridge. It has been this introduction of HPS that has generated an interest in evaluating the adequacy and economic impact of the current AASHTO serviceability limits (Barker & Barth 2007).

## 1.2 Objectives

There are two key objectives for this research effort. The first is to analyze the current AASHTO deflection limits. The second objective is to derive serviceability limits that better control bridge accelerations from excess bridge vibrations and load induced structural deterioration of the concrete deck.

The first objective is analyzing the current AASHTO deflection service criteria. Of particular concern are how the deflection criteria compare with other codes, how the criteria compare to the derived alternative serviceability limits, and the correlation between service level deflections and user comfort and structural damage. The question to answer is whether the current AASHTO Service I limits are adequate in preventing user psychological discomfort and preventing structural damage.

The second objective is to derive alternative serviceability limits that directly control user comfort and prevent structural damage. User comfort is associated with bridge accelerations and, therefore, bridge natural frequency. Flexural deck structural damage is associated with stress and strain of the concrete deck. These are two different properties and, therefore, two different limits will be derived.

In order to better control excess bridge vibrations (user comfort), this research effort aims to derive a formulation based on the bridge natural

frequency. Previous research efforts have tried to use complex modeling of bridge behavior to derive acceptable user comfort criteria (Wright and Walker 1971, Amarakas 1975, and DeWolf and Kou 1997). All of these efforts were unsuccessful in developing acceptable criteria for code purposes. This research effort purposes to use relatively simple modeling of bridge dynamic behavior to obtain a dynamic property that can be used in a user comfort criteria formulation. Additionally, the heavy explanatory nature of existing natural frequency design guides, such as the American Institute of Steel Construction Design Guide 11 (1997), suggests that the typical structural engineer is unfamiliar with natural frequency based design. The proposed user comfort formulation, while based on natural frequency, will be transformed into a formulation utilizing familiar mechanics terms.

User comfort is an every day concern. An occasional violation of user comfort from a rare maximum expected load is unlikely to be of major concern for the bridge user. Additionally, the low occurrence frequency of these maximum service loads warrants not reducing the bridge economy by designing for more conservative loads. This research will utilize the expected daily load for user comfort criteria. In current AASHTO LRFD design specifications, this expected daily load is represented by the fatigue truck load.

To summarize, this research effort will derive a user comfort criteria formulation based on natural frequency while remaining in familiar mechanical terms and utilizing fatigue truck load deflections.

In order to control deformation-induced structural deformation, a second serviceability criteria is formulated that controls the tensile strain in the concrete deck. The criteria will relate the peak negative moment at the piers for continuous span bridges to a limiting tensile strain. As structural deterioration is a maximum load occurrence, the maximum serviceability load is used to calculate the peak negative moment. This maximum service load in the AASHTO LRFD specifications is represented by the Service II loading. Additionally, the tensile stress and strains will be compared to the Service I deflections to determine whether any significant correlation exists between Service I deflections and deck cracking.

### **1.3 Organization**

Chapter 2 further details the history and background of the AASHTO live load deflection limits. Previous studies are presented to better understand the effects of live load deflection criteria with respect to user comfort and structural deterioration and what has been shown to have affects on user comfort and structural damage. Chapter 2 also includes a summary of the 195 bridge database used in this report.

Chapter 3 derives the alternative proposed user comfort serviceability performance design check. Chapter 3 introduces a  $X$  ( $\chi$ ) factor which will serve as the core of the new alternative design limit. The  $X$  factor is a derived term that relates deflection and vibrations. The  $X$  term is correlated to acceptable bridge performance. A set of example calculations are performed using a typical steel girder bridge (Missouri Bridge A6101). The behavior of bridges with as-built properties and loading is analyzed. The method of obtaining bridge behavior at the optimal design state is introduced and described. The results of this optimized procedure are then analyzed for the suite of 195 bridges.

Chapter 4 introduces the proposed limit for preventing structural damage to the concrete deck. The procedure is outlined and results are shown. Again, the suite of bridges is analyzed for the as-built condition and at the optimal design limit state. A relationship is also sought between Service I deflections and strain in the concrete deck.

Chapter 5 provides a summary, conclusions, and recommendations for future work.

## **Chapter 2 Background**

### **2.1 Introduction and Live Load Deflection Criteria**

This chapter provides further background information regarding live load deflections, design criteria, live load deflection studies and natural frequency design.

Deflection limits have their origin from railroad specifications that were an attempt to limit bridge vibration. The 1905 American Railroad Association (AREA) limited the span to depth ratio, which is an indirect method of limiting deflections. In the 1930's, the Bureau of Public Roads performed a study to determine a design method that would limit excess bridge vibration (Barth, Bergman, and Roeder 2002). The study included bridges common for the time period. The bridges consisted of wood plank decks with a superstructure of pony and pin connected trusses, and simple beam bridges. There were no composite beams and few continuous spans. If the building material was steel, ASTM A7 steel was the typical grade. AASHTO deflection limits for bridges first appeared in 1941, partially due to the results of the study (Fountain and Thurman 1987).

The American Society of Civil Engineers investigated the origins for these service load deflection requirements and, in 1958, reported no clear basis for the deflection criteria was found (Barth, Bergman, and Roeder 2002).



Chapter 2 of the AASHTO LRFD design specifications details general design principles. Article 2.5.2.6 advises that the maximum deformation of a bridge should not exceed  $(\text{Span Length})/800$  for general vehicular bridges and for vehicular bridges with pedestrian traffic deformations should not exceed  $(\text{Span Length})/1000$ . The reason for the smaller allowable deflection for the pedestrian bridges is that pedestrians are more sensitive to bridge vibrations than vehicular passengers. AASHTO suggests that the service live load does not exceed the AASHTO HS 20 loading (AASHTO 2002).

## **2.2 Live Load Deflection Studies**

A collection of past research efforts analyze and question the adequacy of the current AASHTO deflection serviceability criteria. A summary of these studies and their conclusions is provided in this section.

Fountain and Thunman (1987) conducted a study which examined live-load deflection criteria for steel bridges with concrete decks. Their study concluded that AASHTO live-load deflection criteria did not achieve the purported goal for strength, durability, safety, or maintenance of steel bridges. The study showed that transverse cracking in the concrete deck slab is the most common form of bridge structural deterioration. The study listed plastic shrinkage, drying shrinkage, deck restraint, long-term flexure under

service loads, and repetitive vibrations from traffic as causes of deck deterioration.

A majority of modern steel-concrete deck slabs are built with a composite design. Fountain and Thunman questioned the AASHTO deflection criteria because of the small flexural tensile stresses in the deck and because the influencing 1930 U.S. Bureau of Public Roads study did not incorporate composite girder bridges. The study also suggests that increased bridge stiffness can cause an increase in deck/beam interaction, thereby increasing the stress acting in the deck (Fountain and Thunman 1987).

Two additional studies (Goodpasture and Goodwin 1971, and Nevels and Hixon 1973) investigated the relation between service deformations and deck deterioration. The studies failed to find any significant correlation.

Wright and Walker (1971) performed a study reviewing the rationality of the deflection limits in regards to the human psychological element and structural deterioration. Human responses to vibrations as well as the affects vibration has on the cracking of the concrete deck were examined. The conclusions of this study are that live-load deflections alone are insufficient in controlling excessive bridge vibration.

Another previous study (Amaraks 1975) used finite element models to determine what properties of bridges and traffic caused excessive vibration. By varying the parameters of span length, stiffness, surface

roughness, axle spacing, number of axles, and vehicle speed, the study was able to determine which parameter affected the maximum acceleration of the bridge the most. From this study it was determined that the largest factor was surface roughness. Span length was another key factor as shorter bridges experienced higher accelerations. Stiffness was a factor, but significantly less than the two previous factors. Vehicle speed was another significant influencing factor on bridge accelerations.

The finding that surface roughness is the largest factor in bridge accelerations was reinforced by another study (Dewolf and Kou 1997). Results from this study examined the effects of vehicle speed, vehicle weight, girder flexibility, deck thickness, and surface roughness on bridge accelerations. The accelerations for a rough surface were 1.75 times the accelerations for a smooth surface. The large impact from vehicle speed on accelerations was also verified in this study.

All of these studies show that the presence of excess vibrations is caused more by the natural frequency of the bridge, vehicle speed, and surface roughness than correlated to the deflection. Deflection limits not considering these factors are insufficient in preventing excess vibrations.

There is a growing movement in structural engineering to move away from simple (span length)/number ratios for serviceability limits. The Ontario Highway Bridge Design Code (1983) does not limit deflection as a

function of only span length; rather the maximum deflection is based on a function of the natural frequency of the bridge. The Ontario Highway Bridge Design Code (OHBC) has three different limit levels: the most conservative is for bridges with heavy pedestrian traffic, a middle level for some pedestrian use, and the most liberal for bridges with no intended pedestrian use. The '96 Australian Bridge Code (1996) also uses a natural frequency based deflection limit (Barth, Christopher, and Wu 2003). In the building structural engineering world, there is a growing movement from the (span length)/number serviceability limit in the current AISC 13<sup>th</sup> ed Steel Design Manual (2005) to a natural frequency method detailed in the AISC Design Guide 11 (1997). While finite element packages and other computer programs can easily compute the modal natural frequencies of a structure, it can be a challenge to properly input the bridge into the model. For these reasons, it is desired to derive a user comfort performance design check that, while based on natural frequency, is in terms well known to the generic bridge engineer.

### **2.3 Bridge Summary**

This study utilizes a suite of 195 steel girder bridges. The bridges come from two sources. Ten of the bridges were used in previous research by Gandiaga (2009). These bridges were selected to have a variation in bridge properties such as span length, girder spacing, steel strength, etc.

Four of these ten bridges utilize high performance steel (HPS). The second source of data was from a database of 185 bridges provided by BridgeTech, Inc. The database contained 126 single span bridges and 59 continuous span bridges. Table 2-1 shows a summary of bridge properties by span. The bridges are located throughout the United States and represent a spectrum of steel girder bridge design.

**Table 2-1 Bridge Database Property Summary**

	1 Span	2 Span	3 Span	4 Span	5 Span	6 Span
Number of Bridges	129	23	10	26	5	1
Span Length Range (ft)	20-205	30-170	38-170	36-173	44-98.5	39-84.75
Steel Strength Range (ksi)	33-50	33-70	33-100	33-50	33-50	36
L/D Range	8.75-42.2	14.3-34.8	16.6-34.6	16.8-33.7	19-23.6	20.8-21.1

Regarding the behavior of interior girder vs. exterior girder behavior, Figure 2-1 shows the natural frequency versus deflection for both interior and exterior girders for simple spans. The quantities in Figure 2-1 will be discussed in later sections. Figure 2-1 is shown here to demonstrate the similarity between interior and exterior girders.

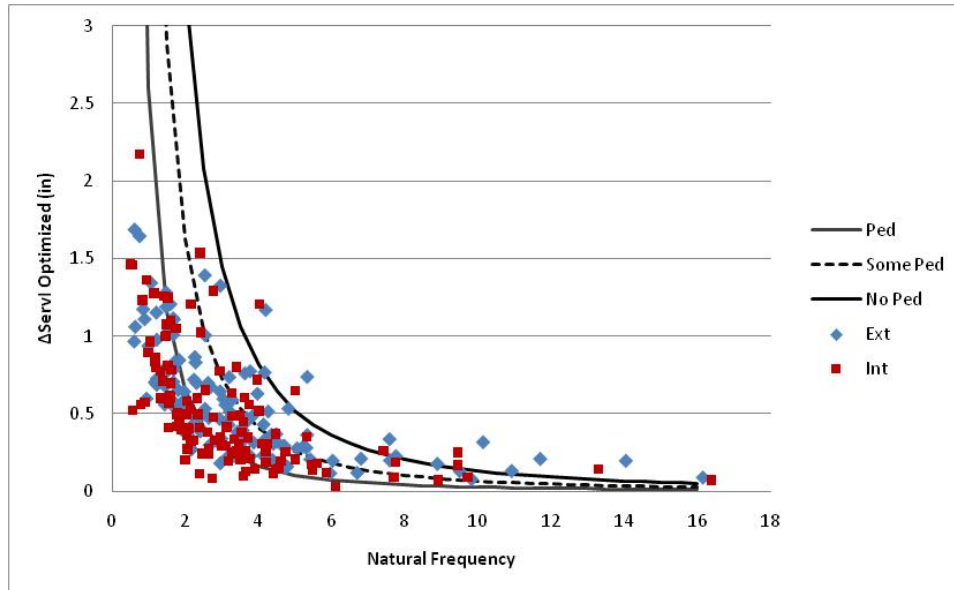


**Figure 2-1 Exterior vs. Interior Girder Behavior Simple Span**

The exterior girders controlled in the majority of bridges. In the interest of brevity and clarity the results shown in this report are for the exterior girders.

## 2.4 Summary

This chapter presented the background for the development of the current AASHTO deflection criteria. The conclusions and information from previous studies are shown. These previous studies reinforce the notion that deflection criteria based on span length alone is insufficient in preventing either user discomfort or structural deterioration. The movement within structural engineering to natural frequency based design criteria is discussed. A description of the bridges used in this study is given. In the next chapter, the user comfort criteria is derived and analyzed.

## **Chapter 3 User Comfort Criteria**

### **3.1 Introduction**

In order to better control excess bridge vibration, the objective is to derive a user comfort serviceability limit based on the natural frequency of the bridge, but formulated in terms familiar to the typical engineer. This chapter derives and analyzes the proposed formulation to control excess vibrations.

### **3.2 Derivation of User Comfort Formulation**

Previous research efforts have tried to use complex modeling of bridge dynamic behavior to derive natural frequency based serviceability criteria (Wright and Walker 1971, Amarak 1975, and DeWolf and Kou 1997). None of these previous efforts have produced acceptable criteria to place in design codes. This study will instead use a simple dynamic pluck test to obtain a dynamic property of the bridge, which, in turn, is used to formulate the proposed user comfort serviceability criteria.

#### **3.2.1 Dynamic Pluck Test**

In the dynamic pluck test, the bridge is loaded with the fatigue truck at the location that incurs maximum deflection. The load is then removed

instantaneously, and free vibration is allowed. The response is then correlated to acceptable vibration for steel girder bridges..

Dynamics of the bridge pluck test gives the following relation:

$$\ddot{u}_{max} = \Delta_{max} \cdot \omega_n^2 \quad (\text{Eqn 3-1})$$

where

$\ddot{u}_{max}$  = maximum acceleration,

$\Delta_{max}$  = initial deflection, in this model the initial deflection is the maximum deflection caused by the fatigue truck load, and

$\omega_n$  = bridge circular natural frequency.

The acceleration term “ $\ddot{u}$ ” is defined as being some maximum percentage times the acceleration of gravity:

$$\ddot{u}_{max} = \alpha_{max} \cdot g \quad (\text{Eqn 3-2})$$

where

$\alpha_{max}$  = maximum percentage of acceleration of gravity, and

$g$  = acceleration of gravity.

The relation between circular natural frequency and the natural frequency is given as:

$$\omega_n = 2\pi \cdot f_n \quad (\text{Eqn 3-3})$$

where

$f_n$  = natural frequency of the bridge.



Substitution of the maximum acceleration, Equations 3-2, and the natural circular frequency, Equation 3-3, into Equation 3-1 yields:

$$a_{max} \cdot g = \Delta_{max} \cdot (2\pi \cdot f_n)^2 \quad (\text{Eqn 3-4})$$

which after performing the squaring operation becomes:

$$a_{max} \cdot g = 4 \cdot \Delta_{max} \cdot \pi^2 \cdot f_n^2 \quad (\text{Eqn 3-5})$$

where the natural frequency of a simply supported, single span bridge  $f_{n, sb}$  is given as:

$$f_{n, sb} = \frac{\pi}{2 \cdot L^2} \cdot \sqrt{\frac{E \cdot I_b \cdot g}{W}} \quad (\text{Eqn 3-6})$$

where

$L$  = span length,

$E$  = modulus of elasticity,

$I_b$  = moment of inertia at midspan,

$g$  = acceleration of gravity, and

$w$  = weight per unit length of bridge girder.

The natural frequency of a continuous girder,  $f_{n, cs}$ , is as defined by:

$$f_{n, cs} = c_n \cdot f_{n, sb} \quad (\text{Eqn 3-7})$$

where

$c_n$  = continuous span correction factor, and

$f_{n, sb}$  = single span natural frequency.

In this research effort, the continuous span correction factor is defined to be equal to the correction factor  $\lambda^2$  defined by Wu (2003) as:

$$c_n = \lambda^2 = a \cdot \frac{I_{avg}^c}{L_{max}^b} \quad (\text{Eqn 3-8})$$

where

$I_{avg}$  = average moment of inertia of composite girder,

$L_{max}$  = maximum span length, and

$a, b, c$  are coefficients given in Table 3-1 below.

**Table 3-1  $\lambda^2$  Coefficients**

Number of Spans	a	b	c
2	0.9539	0.04586	0.03176
3 or more	0.8785	-0.03311	0.03348

Note that for a single span bridge the correction factor  $c_n$  can simply be set equal to one. Additionally, any appropriate method used to determine the correction factor to transform the single span natural frequency to the continuous span natural frequency may substitute the  $\lambda^2$  method detailed in this study.

The definition of the natural frequency thus becomes:

$$f_n = \frac{c_n \cdot \pi}{2 \cdot L^2} \cdot \sqrt{\frac{E \cdot I_p \cdot g}{W}} \quad (\text{Eqn 3-9})$$

Substitution of the natural frequency equation into Equation 3-6 yields

Equation 3-10:

$$\alpha_{max} \cdot g = 4 \cdot \Delta_{max} \cdot \pi^2 \cdot \left( \frac{c_N \cdot \pi}{2 \cdot L^2} \cdot \sqrt{\frac{E \cdot I_b \cdot g}{W}} \right)^2 \quad (\text{Eqn 3-10})$$

Which simplifies to:

$$\alpha_{max} \cdot g = \frac{\Delta_{max} \cdot \pi^4 \cdot c_N^2 \cdot E \cdot I_b \cdot g}{L^4 \cdot W} \quad (\text{Eqn 3-11})$$

The solution of Equation 3-11 for  $\Delta_{max}$  yields Equation 3-12:

$$\Delta_{max} = \left( \frac{\alpha_{max}}{\pi^4} \right) \cdot \left( \frac{W \cdot L^4}{c_N^2 \cdot E \cdot I_b} \right) \quad (\text{Eqn 3-12})$$

This dynamic pluck test is a simplified model of the bridge's dynamic response and behavior. The maximum accelerations given by this pluck test are not going to be equivalent to the accelerations experienced by the bridge users in actual conditions; therefore, it is not appropriate to use developed acceptable acceleration criteria for this method. The  $\alpha_{max}$  must be calibrated to an appropriate level; however, in interest of simplifying the formulation, all constant terms are included into one factor X (chi). Calibration of this X factor directly results in the calibration of  $\alpha_{max}$ . Equation 3-13 defines the X factor term as:

$$X = \frac{\alpha_{max}}{\pi^4} \quad (\text{Eqn 3-13})$$

Substitution of the X factor yields Equation 3-16:

$$\Delta_{\max} = X \cdot \frac{W \cdot L^4}{c_n^2 \cdot E \cdot I_b} \quad (\text{Eqn 3-16})$$

This equation is very similar to deflection equations currently used by structural engineers. By rearranging Equation 3-16, the X factors can be calculated based on deflection as shown in Equation 3-17 below.

$$X = \frac{\Delta_{\max} c_n^2 \cdot E \cdot I_b}{W \cdot L^4} \quad (\text{Eqn 3-17})$$

This Equation can be used to determine as-built and design optimized X factors for the database bridges. With these derived relations, it is now possible to formulate a user comfort design criteria. The percentage of gravity,  $\alpha_{\max}$ , is limited to some maximum allowable percentage,  $\alpha_{\text{lim}}$ . This term is within the X factor, and a new limiting X factor term,  $X_{\text{lim}}$ , is defined as:

$$X_{\text{lim}} = \frac{\alpha_{\text{lim}}}{\pi^4} \quad (\text{Eqn 3-18})$$

The maximum allowable deflection,  $\Delta_{\text{Allow}}$ , is calculated as:

$$\Delta_{\text{Allow}} = \left( \frac{\alpha_{\text{lim}}}{\pi^4} \right) \cdot \left( \frac{W \cdot L^4}{c_n^2 \cdot E \cdot I_b} \right) \quad (\text{Eqn 3-19})$$

which using the definition of the limiting X factor,  $X_{\text{lim}}$ , becomes Equation 3-20.

$$\Delta_{\text{Allow}} = (X_{\text{lim}}) \cdot \left( \frac{W \cdot L^4}{c_n^2 \cdot E \cdot I_b} \right) \quad (\text{Eqn 3-20})$$

This research study proposes that the maximum deflection resulting from the daily expected load, the fatigue truck loading,  $\Delta_{\text{fat}}$ , to be used in the

user comfort formulation. This deflection is modeled similar to the fatigue load distribution for the current AASHTO fatigue design check. The bridge is loaded with a single truck without the multiple presence factor. The maximum fatigue truck load induced deflection can be defined as.

$$\Delta_{fat} = 0.75 g_m \cdot (1 + i) \Delta_{fat\_1girder} \quad (\text{Eqn 3-21})$$

Where

$g_m$  = controlling moment load distribution factor for single lane loaded,

$i$  = fatigue impact factor

$\Delta_{fat\_1girder}$  = deflection induced by whole fatigue truck load on a single girder.

This maximum fatigue truck deflection must be less than or equal to the allowable deflection. The serviceability design limit becomes:

$$\Delta_{fat} \leq \Delta_{Allow} = (X_{lim}) \cdot \left( \frac{w \cdot L^4}{c_n^2 \cdot E \cdot I_b} \right) \quad (\text{Eqn 3-22})$$

where

$\Delta_{Allow}$  = maximum allowable deflection,

$\Delta_{fat}$  = deflection from the AASHTO fatigue truck loading,

$w$  = weight per unit length of bridge girder,

$L$  = span length,

$I_b$  = transformed short term composite moment of inertia at midspan,

$E$  = modulus of elasticity of steel,

$c_n$  = natural frequency correction factor for continuous span bridges, and

$X_{lim}$  = limiting X factor.

The resulting serviceability design limit uses the natural frequency to control user comfort; however it is formulated to appear as a deflection limit. While the formulation of the above serviceability criterion is proposed, the limiting X factor,  $X_{lim}$ , requires additional future research and calibration to determine the final appropriate values. This calibration process will involve analyzing existing bridges with recorded acceptable and unacceptable bridge vibration behavior. For demonstration purposes this research correlates  $X_{lim}$  to the 1983 OHBC natural frequency criteria.

### **3.2.2 Correlating $X_{lim}$ to the OHBC Criteria**

#### **3.2.2.1 OHBC Criteria**

The Ontario Highway Bridge Design Code (1983) uses a relationship between static deflection and the first flexural natural frequency of the bridge for their user comfort serviceability criteria. There are three levels of serviceability depending on the level of intended pedestrian use: no intended pedestrian use, some intended pedestrian use, and heavy intended pedestrian use. Figure 3-1 shows the OHBC's limit relationship between static deflection and first natural frequency. The units have been converted to US units here.

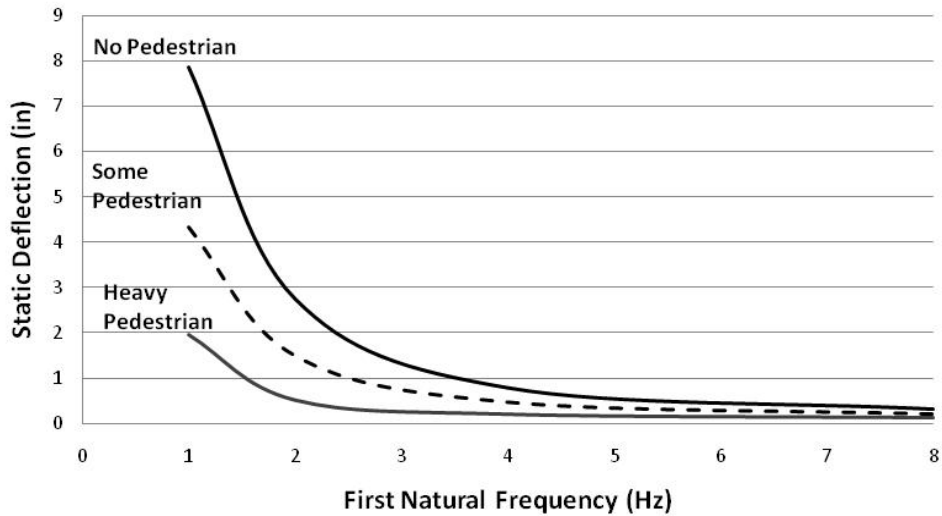


**Figure 3-1 Ontario Bridge Code Natural Frequency vs. Maximum Allowable Deflection (OHBC 1983)**

A power function was approximated for the relationship between the first natural flexural frequency,  $f_n$ , and the static deflection for the three levels of intended pedestrian use in the Ontario code. The basic form of the function that approximates the relation is given by Equation 3-23.

$$\Delta_{allow,i} = \frac{A_i}{f_n^2} \quad (\text{Eqn 3-23})$$

where the  $A_i$  term is a constant and the “i” term denotes the level of pedestrian use. For bridges with little to no pedestrian traffic the  $A_i$  constant is  $A_{no\_ped}$ , while for bridges with some intended pedestrian traffic the constant is  $A_{some\_ped}$  and for bridges with large intended pedestrian use the constant is  $A_{ped}$ . Since these values were derived for limiting deflections in units of inches, the unit associated with the A values in this chapter are inches cycles squared per second squared as shown below.

$$A_{\text{limits}} = \frac{111 \cdot \text{cycles}^2}{s^4}$$

After performing iterations, an  $A_{\text{no\_ped}} = 13$  approximates the limiting relation between deflection and the first natural frequency of the bridge. This yields the following relation for a bridge with little to no intended pedestrian usage.

$$\Delta_{\text{Allow, no\_ped}} = \frac{13}{f_n^2} \quad (\text{Eqn 3-24})$$

It was decided to make  $A_{\text{some\_ped}}$  and  $A_{\text{ped}}$  a percentage of  $A_{\text{no\_ped}}$ . By performing several iterations an  $A_{\text{some\_ped}}$  term equal to 50 percent of the  $A_{\text{no\_ped}}$  value of 13 approximates the some pedestrian traffic limit relationship found in the Ontario Code. This yields an  $A_{\text{some\_ped}}$  equal to 6.5 and the following relation shown below.

$$\Delta_{\text{Allow, some\_ped}} = 6.5 \frac{1}{f_n^2} \quad (\text{Eqn 3-25})$$

An  $A_{\text{ped}}$  term equal to 20 percent of the  $A_{\text{no\_ped}}$  value of 13 approximates the heavy pedestrian traffic limit relationship found in the Ontario Code. This yields an  $A_{\text{ped}}$  equal to 2.6 and the following relation shown below.

$$\Delta_{\text{Allow, ped}} = 2.6 \frac{1}{f_n^2} \quad (\text{Eqn 3-26})$$



These approximation relations are plotted against the actual Ontario Bridge Code user comfort serviceability limits in Figure 3-2. Figure 3-3 shows the same relations using a log-log scale.

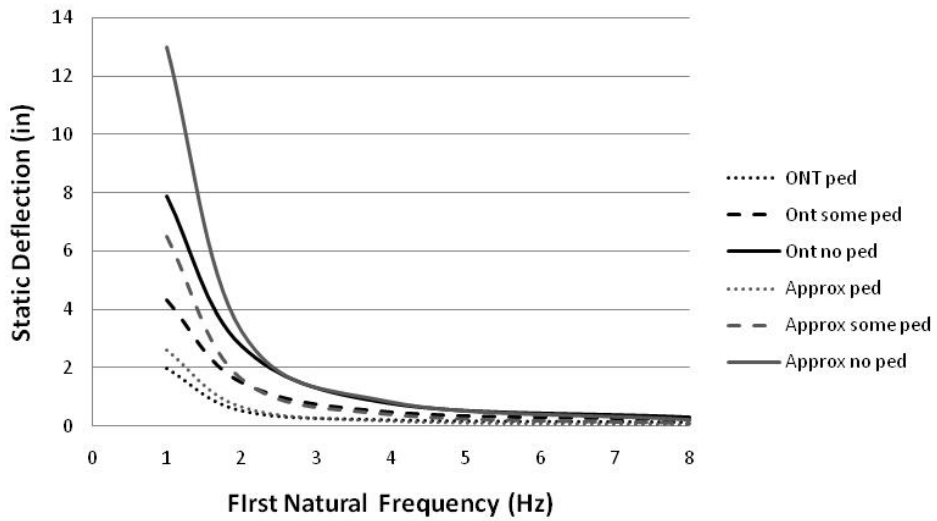


**Figure 3-2 Approximate & Actual Deflection vs. 1st Natural Frequency**

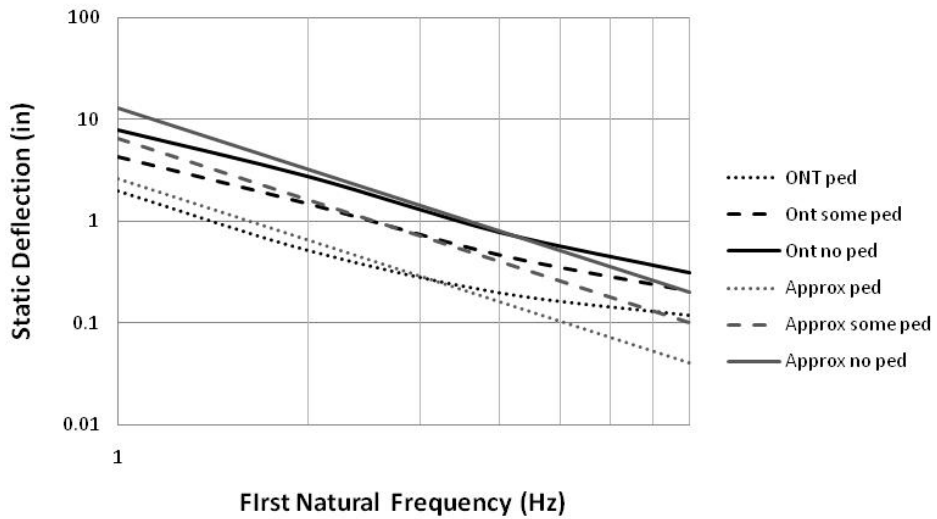


**Figure 3-3 Approximate & Actual Deflection vs. 1st Natural Frequency Log-Log Axis**

From these figures it is apparent that for natural frequencies less than 2 Hz, the approximated relations allow for higher deflections than the deflections allowed by the Ontario Bridge Code. In other words, the approximate relations are less conservative than the Ontario Bridge Code for natural frequencies of less than approximately 2 Hz. This difference is tolerated because the limiting deflections for bridges with frequencies lower than 2 Hz are high enough in value that it is unlikely for an actual bridge to achieve this deflection as stresses for other limit states would prohibit such high deflection. This is more clearly seen when plotting the calculated as-built first natural frequencies of the bridges in this study. The range of natural frequency where a deflection limit is likely to control is in bridges with natural frequencies of 2 Hz or greater. It is in this range of natural frequencies that it was deemed more crucial in closely approximating the given relation between first natural frequencies and limiting deflection.

### **3.2.2.2 Correlating $X_{lim}$ to OHBC Criteria**

The power functions applied in the previous section approximate the user comfort serviceability limits found in the Ontario Highway Bridge Code. However, these limits still require the calculation of the natural frequency of a bridge. In order to correlate the  $X_{lim}$  method to the OHBC criteria, the relationship between natural frequency and  $X$  is required.

The equation for the first flexural frequency is recalled.

$$f_N = \frac{c_N \cdot \pi}{2 \cdot L^2} \cdot \sqrt{\frac{E \cdot I_B \cdot g}{W}} \quad (\text{Eqn 3-27})$$

Therefore the squared first flexural frequency is given by the squaring the above equation.

$$f_N^2 = \frac{c_N^2 \cdot \pi^2}{4 \cdot L^4} \cdot \frac{E \cdot I_B \cdot g}{W} \quad (\text{Eqn 3-28})$$

Substituting the squared natural frequency equation into the function relating the first flexural frequency to the static deflection, Equation 3-23, yields the following.

$$\Delta_{\text{allow}} = \frac{A_t}{\frac{c_N^2 \cdot \pi^2}{4 \cdot L^4} \cdot \frac{E \cdot I_B \cdot g}{W}} \quad (\text{Eqn 3-29})$$

This equation is rearranged as

$$\frac{\Delta_{\text{allow}} \cdot c_N^2 \cdot E \cdot I_B \cdot \pi^2 \cdot g}{W \cdot L^4} = A_t$$

Recalling the definition of the X factor from Equation 3-20 and substituting in the definition of  $X_{\text{lim}}$  into the above relation,

recall:

$$X_{\text{lim}} = \frac{\Delta_{\text{allow}} \cdot c_N^2 \cdot E \cdot I_B}{W \cdot L^4}$$

and substituting:

$$X_{\text{lim}} \cdot \frac{\pi^2 \cdot g}{4} = A_t$$

the maximum limiting X factor is given by:

$$X_{lim} = \frac{4A_i}{\pi^2 \cdot g} \quad (\text{Eqn 3-30})$$

where  $A_i$  is equal to 2.6 for bridges with heavy pedestrian traffic, 6.5 for bridges with some pedestrian traffic, and 13.0 for bridges with little to no pedestrian traffic. These  $X_{lim}$  values are then substituted into Equation 3-20 to yield the limiting deflection. Since  $X_{lim}$  is not a function of any other particular structural property of a bridge, there will be a constant  $X_{lim}$  for each three levels of pedestrian use. These are shown in Table 3-2 below.

**Table 3-2  $X_{lim}$  for Various Levels of Anticipated Pedestrian Use**

Level of Pedestrian Traffic	$X_{lim}$
Little to None	0.01370
Some Pedestrian	0.00685
Heavy	0.00274

Using the Ontario Code user comfort serviceability criteria to correlate the proposed Equation 3-22 criteria, the following equations would be used to limit fatigue deflections for control of user comfort:

$$\Delta_{fat} \leq \Delta_{Allow, no_{ped}} = X_{lim, no_{ped}} \cdot \frac{W \cdot L^4}{C_n^2 \cdot E \cdot I_b} \quad (\text{Eqn 3-31})$$

$$\Delta_{fat} \leq \Delta_{Allow, some_{ped}} = X_{lim, some_{ped}} \cdot \frac{W \cdot L^4}{C_n^2 \cdot E \cdot I_b} \quad (\text{Eqn 3-32})$$

$$\Delta_{fat} \leq \Delta_{Allow, ped} = X_{lim, ped} \cdot \frac{W \cdot L^4}{C_n^2 \cdot E \cdot I_b} \quad (\text{Eqn 3-33})$$

Although the formulation of the equations are proposed, additional research is necessary to fully calibrate and finalize the appropriate  $X_{lim}$  values for each level of intended pedestrian use.

### **3.3 Sample Calculations Using Missouri Bridge A6101**

In this section, Missouri Bridge A6101 is used in sample calculations that show the methods used in this research effort. For further information about Missouri Bridge A6101, the reader is referred to Gandiaga (2009). These same calculations were performed for each of the 195 bridges in the bridge suite. The calculations are for the bridge with the loads as per the 2002 AASHTO LRFD design criteria, these loads will be referred to as the as-built loads.

#### **3.3.1 Calculating Bridge Properties**

This section shows the methods used to calculate the properties required to determine the deflections, natural frequencies, and X factors used in this research effort.

##### **3.3.1.1 Calculating the Distributed Weight (w)**

The effective weight of the girder is assumed to compose of the weight of the steel substructure, the concrete haunch, the concrete deck, and the wearing surface. The weight of the sidewalks and barriers are not

considered, as neglecting the mass of the curb, railing, and sidewalk results in a lower weight. This lower weight results in a higher natural frequency and lower allowable maximum deflections. Therefore, neglecting the weight of the sidewalk, curb, and railing produces conservative results. The steel substructure is assumed to consist of the steel girder with an additional 5% of the steel girder weight to account for other steel components such as stiffeners, bracing, diaphragms, etc. The concrete deck and wearing surface are assumed to be distributed by tributary areas. The haunch is also considered. The total load of the girder is then divided by the total length to give an average distributed weight of the composite girder.

The girder layout of one span of Missouri Bridge A6101 consists of two steel cross sections of varying size. Table 3-3 below shows the cross sectional areas of the top flange, web, bottom flange, and the total cross sectional area with weight per foot for the gross steel section.

**Table 3-3 Steel Section Distributed Weight Properties**

Steel Section	Top Flange Area (in <sup>2</sup> )	Web Area (in <sup>2</sup> )	Bottom Flange Area (in <sup>2</sup> )	Gross Section Area (ft <sup>2</sup> )	Weight (kip/ft)	Length (ft)
1	9.92	27.88	12.87	0.352	0.172	95.8
2	25.79	30.18	25.79	0.568	0.278	41.7

$$\gamma_{\text{steel}} = 0.49 \text{ kip/ft}^3$$

The distributed weights of the different steel section are averaged in order to come up with an average distributed weight to be used in calculating the natural frequencies of the bridge. The average distributed weight for the steel girder is as follows:

$$W_{\text{st}} = \frac{\sum_{i=1}^n w_i \cdot L_i}{\sum_{i=1}^n L_i} = \frac{(0.172 \cdot 95.8 + 0.278 \cdot 41.7) \text{kip}}{95.8 \text{ft} + 41.7 \text{ft}} = \frac{0.204 \text{kip}}{\text{ft}}$$

where:

$w_i$  = distributed weight of the  $i$ th steel section,

$L_i$  = length of the  $i$ th steel section,

$n$  = number of different girder cross sections use.

The concrete haunch also varies coincidentally with the steel sections. Table 3-3 below gives the dimensions, areas, distributed weights and length of each haunch section.

**Table 3-4 Concrete Haunch Distributed Weight Properties**

Haunch Section	Thickness (in)	Breadth (in)	Haunch Area (in <sup>2</sup> )	Haunch Area (ft <sup>2</sup> )	Weight (kip/ft)	Length (ft)
1	1.77	12.60	22.32	0.155	0.023	95.8
2	1.30	20.47	25.79	0.179	0.027	41.7

$$\gamma_{\text{con}} = 0.15 \text{ kip/ft}^3$$

The distributed weight of the concrete haunch is calculated in a manner similar to the distributed weight of the steel girder.

$$W_{concrete} = \frac{\sum_{i=1}^n w_i \cdot L_i}{\sum_{i=1}^n L_i} = \frac{(0.023 \cdot 95.8 + 0.027 \cdot 41.7)kip}{95.8ft + 41.7ft} = \frac{0.0242kip}{ft}$$

where:

$w_i$  = distributed weight of the  $i$ th concrete haunch section,

$L_i$  = Length of the  $i$ th concrete haunch section, and

$n$  = number of different haunch cross sections use.

The concrete slab section is constant across the span; the distributed weight of the concrete deck is:

$$W_{concrete} = t_s \cdot b_{eff} \cdot \gamma_{conc} = \frac{8.66tn}{12in/ft} \cdot 8.686ft \cdot \frac{0.150kip}{ft} = \frac{0.940kip}{ft}$$

where:

$t_s$  = depth of the concrete slab,

$b_{eff}$  = effective width of concrete slab, and

$\gamma_{conc}$  = unit weight of concrete.

The wearing surface distribution is assumed constant across the span.

The calculation of the distributed weight of the wearing surface is as follows:

$$W_{ws} = p_{ws} \cdot b_{eff} = 0.038ksf \cdot 8.686ft = \frac{0.330kip}{ft}$$

where:

$p_{ws}$  = estimated load of the wearing surface, and

$b_{eff}$  = effective width of concrete slab.



The sum of the calculated distributed weights gives the total distributed length of the girder as shown below.

$$W = 1.05 \cdot W_{\text{slab}} + W_{\text{concrete}} + W_{\text{concrete}} + W_{\text{steel}}$$

$$W = 1.05 \cdot 0.204 \frac{\text{kip}}{\text{ft}} + 0.0242 \frac{\text{kip}}{\text{ft}} + 0.940 \frac{\text{kip}}{\text{ft}} + 0.330 \frac{\text{kip}}{\text{ft}}$$

$$W = \frac{1.51 \text{kip}}{\text{ft}}$$

### 3.3.1.2 Midspan Moment of Inertia

The moment of inertia is the short term composite moment of inertia since the sought properties are short term deflections. The section of interest is the section at the point of maximum deflection for a span, generally either located approximately at 40% or 50% of the span. The components that contribute to the moment of inertia are the steel girder, the concrete haunch, and the effective width and thickness of the concrete deck. The short term composite moments of inertia were provided within the database. Even if a bridge is designed as noncomposite, the composite properties are used because noncomposite bridges act compositely at service loads. The short term composite moment of inertia at midspan for Missouri Bridge A6101 is:

$$I_B = 70678 \text{in}^4.$$

### 3.3.1.3 Calculating $c_n$

The continuous span correction factor transforms the natural frequency for a single span bridge to the continuous span natural frequency. Any appropriate engineering method may be used to determine this correction factor. This research effort uses the  $\lambda^2$  method derived by Wu (2003). For simple spans, the correction factor is equal to one. For continuous spans, the longest span length is used for  $L_{\max}$ , while the coefficients a, b, and c, are all taken from Table 3-1 and are dependent on the number of spans. The average moment of inertia is taken as the average of the short term composite moment of inertia including concrete. The correction factor is then computed using Equation 3-8.

The calculation of the  $\lambda^2$  correction factor requires the average moment of inertia, number of spans, and the maximum span length. The average moment of inertia is calculated in a similar manner to the distributed weights:

$$I_{avg} = \frac{\sum_{i=1}^n I_i \cdot L_i}{\sum_{i=1}^n L_i} = \frac{78678 \text{ in}^4 \cdot 95.8 \text{ ft} + 118800 \text{ in}^4 \cdot 41.7 \text{ ft}}{95.8 \text{ ft} + 41.7 \text{ ft}} = 90840 \text{ in}^4$$

Missouri Bridge A6101 is a two span bridge, therefore from Table 3-1 coefficients a, b, and c are:

$$a = 0.9539,$$

$$b = 0.04586, \text{ and}$$

$$c = 0.03176 .$$

Missouri Bridge A6101 has two spans of equal length of 137.5ft.

The correction factor is thus:

$$\lambda^S = \alpha \cdot \frac{I_{avg}^S}{L_{max}^S} = 0.9539 \cdot \frac{90840^{0.09176}}{137.5^{0.04396}} = 1.094$$

$$c_n = \lambda^S = 1.094$$

### 3.3.2 Sample Calculations for Deflections

This study proposes to use the fatigue truck loading for user comfort serviceability criteria. The LRFD Fatigue Truck (AASHTO 2002) is a single HL-93 truck with constant axle spacing of 30.0ft between the rear 32kip axles, an impact factor of 0.15, and a load factor of 0.75 (see AASHTO LRFD 3.6.1.4.1 and AASHTO LRFD Table 3.4.1-1 Load Combination and Load Factors). Equation 3-21 is used to calculate the deflection from a single fatigue truck of a girder.

While not proposed for use within the user comfort criteria, this study does use the Service I deflections for analysis purposes. The method for calculating the LRFD Service I deflections is detailed in Gandiaga (2009).

The following deflection values are sought: the LRFD optional deflection from Service I loads,  $\Delta_{SerI}$ , the deflection from a fatigue truck loading,  $\Delta_{fat}$ , the AASHTO Service I maximum allowable deflection,  $\Delta_{Allow,SerI}$ , and the allowable deflection for the proposed  $X_{lim}$  method. The

results for calculating the deflections for Service I level loading are shown below:

$$\Delta_{\text{serv}} = DF_{\Delta} \cdot \Delta_{LL+IM} = 0.51 \cdot 2.59 \text{ in} = 1.321 \text{ in}$$

$$\Delta_{\text{allow, serv}} = \frac{L}{800} = \frac{1654 \text{ in}}{800} = 2.07 \text{ in}$$

The deflection from a total fatigue truck loading on a single girder for Missouri Bridge A6101 is:

$$\Delta_{\text{fat, girder}} = 1.370 \text{ in}$$

Equation 3-21 is then used to calculate the deflection from the distributed fatigue truck loading. The controlling single lane moment distribution factor is used and a fatigue impact factor of 0.15 is used.

$$\Delta_{\text{fat}} = 0.75 g_m \cdot (1 + I) \Delta_{\text{fat, girder}}$$

$$\Delta_{\text{fat}} = 0.75 \cdot 0.464 \cdot (1 + 0.15) \cdot 1.370 \text{ in}$$

$$\Delta_{\text{fat}} = 0.549 \text{ in}$$

The allowable deflections as per the  $X_{\text{lim}}$  method are calculated using Equations 3-31 through 3-32 using the  $X_{\text{lim}}$  values from Table 3-2, and the previously calculated properties:  $w$ ,  $c_n$ , and  $I_b$ , and the span length,  $L$ .

$$\Delta_{\text{allow, no ped}} = X_{\text{lim, no ped}} \cdot \frac{w \cdot L^4}{c_n^2 \cdot E \cdot I_b}$$

$$\Delta_{\text{allow, no ped}} = 0.01370 \cdot \frac{1.51 \text{ kip} \cdot (137.5 \text{ ft})^4 \cdot \frac{1728 \text{ in}^3}{\text{ft}^3}}{1.094^2 \cdot 29000 \text{ ksi} \cdot 78678 \text{ in}^4}$$

$$\Delta_{\text{allow, no ped}} = 4.68 \text{ in}$$

$$\Delta_{\text{Allow, some ped}} = X_{\text{lim, some ped}} \cdot \frac{w \cdot L^4}{c_n^2 \cdot E \cdot I_b}$$

$$\Delta_{\text{Allow, some ped}} = 0.00685 \cdot \frac{\frac{1.51 \text{ kip}}{\text{ft}} \cdot (137.5 \text{ ft})^4 \cdot \frac{1728 \text{ in}^3}{\text{ft}^3}}{1.094^2 \cdot 29000 \text{ ksi} \cdot 78678 \text{ in}^4}$$

$$\Delta_{\text{Allow, some ped}} = 2.34 \text{ in}$$

$$\Delta_{\text{Allow, ped}} = X_{\text{lim, ped}} \cdot \frac{w \cdot L^4}{c_n^2 \cdot E \cdot I_b}$$

$$\Delta_{\text{Allow, ped}} = 0.00274 \cdot \frac{\frac{1.51 \text{ kip}}{\text{ft}} \cdot (137.5 \text{ ft})^4 \cdot \frac{1728 \text{ in}^3}{\text{ft}^3}}{1.094^2 \cdot 29000 \text{ ksi} \cdot 78678 \text{ in}^4}$$

$$\Delta_{\text{Allow, ped}} = 0.936 \text{ in}$$

### 3.3.3 Sample Natural Frequency Calculations

This research effort uses the natural frequency of bridges for analytical purposes. Using Equation 3-9 and the previously calculated values of distributed girder weight,  $w$ , midspan moment of inertia short term composite,  $I_b$ , the continuous span correction factor,  $c_n$ , and the given values of span length,  $L$ , modulus of elasticity of steel,  $E$ , and the acceleration of gravity,  $g$ , the natural frequency for Missouri Bridge A6101 is:

$$f_n = \frac{c_n \cdot \pi}{2 \cdot L^2} \cdot \sqrt{\frac{E \cdot I_b \cdot g}{w}}$$

$$f_n = \frac{1.094 \cdot \pi}{2 \cdot (137.5 \text{ ft})^2} \cdot \sqrt{\frac{29000 \text{ ksi} \cdot 78678 \text{ in}^4 \cdot \frac{386 \text{ in}}{\text{s}^2}}{\frac{1.51 \text{ kip}}{\text{ft}}}}$$

$$f_n = 1.67\text{Hz}$$

### 3.3.4 Sample X Factor Calculations

As-built X factors can be back-calculated using Equation 3-17.

These back-calculated X factors are used for analytical purposes within this study.

$$X_{\text{SerI}} = \frac{\Delta_{\text{SerI}} \cdot c_n^2 \cdot E \cdot I_b}{w \cdot L^4} = \frac{1.321\text{in} \cdot 1.094^2 \cdot 29000\text{kst} \cdot 78678\text{in}^4}{1.51 \text{kip/ft} \cdot (137.5\text{ft})^4 \cdot 1728\text{in}^3/\text{ft}^3} = 0.0038$$

$$X_{\text{Allow,SerI}} = \frac{\Delta_{\text{Allow,SerI}} \cdot c_n^2 \cdot E \cdot I_b}{w \cdot L^4} = \frac{2.07\text{in} \cdot 1.094^2 \cdot 29000\text{kst} \cdot 78678\text{in}^4}{1.51 \text{kip/ft} \cdot (137.5\text{ft})^4 \cdot 1728\text{in}^3/\text{ft}^3} = 0.0060$$

$$X_{\text{fat}} = \frac{\Delta_{\text{fat}} \cdot c_n^2 \cdot E \cdot I_b}{w \cdot L^4} = \frac{0.349\text{in} \cdot 1.094^2 \cdot 29000\text{kst} \cdot 78678\text{in}^4}{1.51 \text{kip/ft} \cdot (137.5\text{ft})^4 \cdot 1728\text{in}^3/\text{ft}^3} = 0.0016$$

## 3.4 Results for Bridges with As-Built Loading

The calculations detailed in Section 3.3 were applied to the suite of 195 bridges with the as-built loading. The results of these calculations are shown and analyzed within this section.

### 3.4.1 Service I Deflections

In order to gain a better understanding of the behavior of the bridges with regards to the current AASHTO deflection criteria, the Service I as-built

deflections are plotted against the span length for simple spans in Figure 3-4 and continuous spans in Figure 3-5. The figures also show the plotted allowable deflection limits for the current AASHTO criteria.

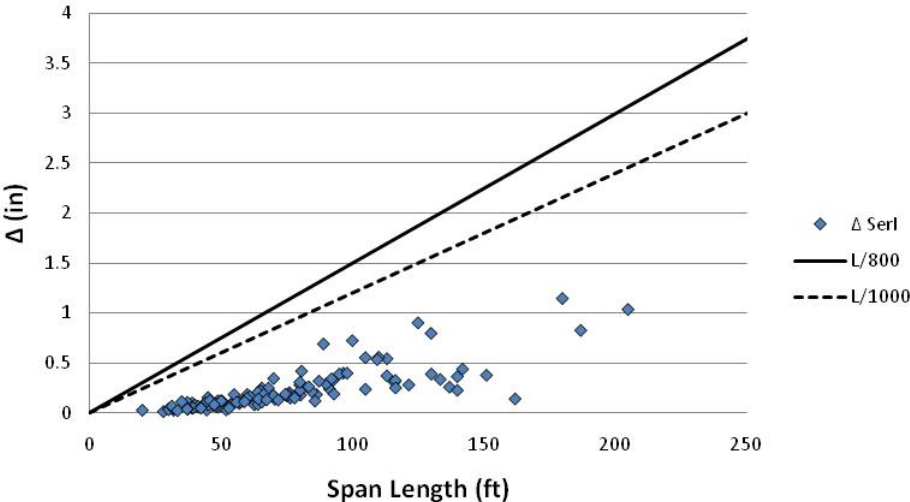


**Figure 3-4 Service I Deflections vs. Span Length Simple Spans**

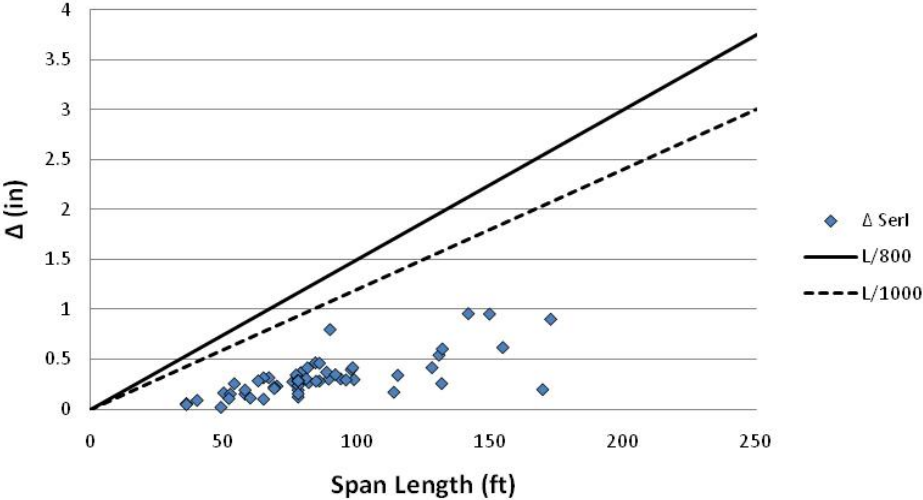


**Figure 3-5 Service I Deflections vs. Span Length Continuous Spans**

These figures clearly show that the bridges all meet the current AASHTO Service I criteria. Therefore, if the current criterion adequately controls bridge vibrations and structural deterioration, these bridges should not have user comfort or load-induced structural deterioration problems.

### **3.4.2 Fatigue Deflections**

In order to gain a better understanding of the behavior of the bridges with respect to fatigue deflections, the as-built fatigue deflections are plotted compared to span length. Since the  $L/800$  and  $L/1000$  deflection limits are correlated to the Service I deflections, it is not appropriate to compare the fatigue deflection to these limits. Instead the deflection criterion is multiplied by the average of the ratio of fatigue to Service I deflections. This ratio method is used because two different distribution factors are used to calculate the fatigue deflections compared to the Service I deflections. This prevents simply being able to scale the Service I deflection limits. The fatigue as-built deflections are plotted against span length for simple spans in Figure 3-6 and continuous spans in Figure 3-7.



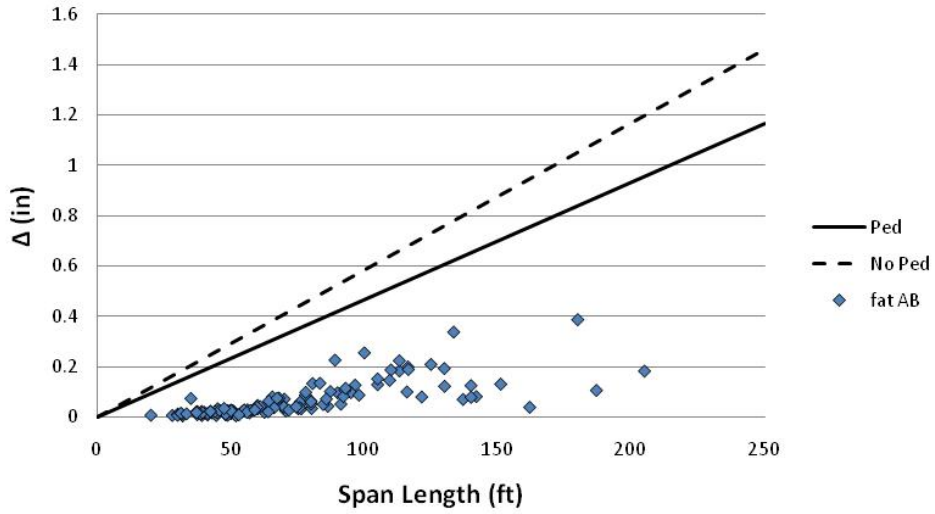


**Figure 3-6 Fatigue Deflections vs. Span Length Simple Spans**

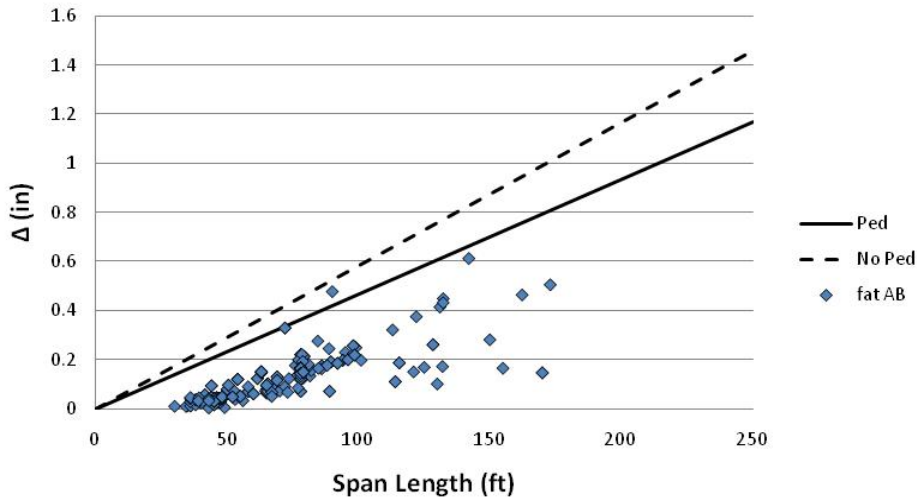


**Figure 3-7 Fatigue Deflections vs. Span Length Continuous Spans**

These figures show similar behavior as the previous Service I deflection figures in Section 3.4.1. All of the bridges meet the criteria for the no pedestrian limit, while the majority of bridges meet the pedestrian limit.

The fatigue deflections are plotted versus the bridge natural frequencies in order to analyze this relation. Figure 3-8 shows the fatigue deflections versus natural frequency for simple span bridges and Figure 3-9 shows the same relation on a log-log scale. Figure 3-10 shows the fatigue deflections versus natural frequency for continuous spans, and Figure 3-11 shows the same relation with a log-log axis. These figures also include the approximate functions relating maximum deflection to natural frequency, Equations 3-24 through 3-26. A data point above this line indicates a violation of the criteria for a particular level of intended pedestrian use.

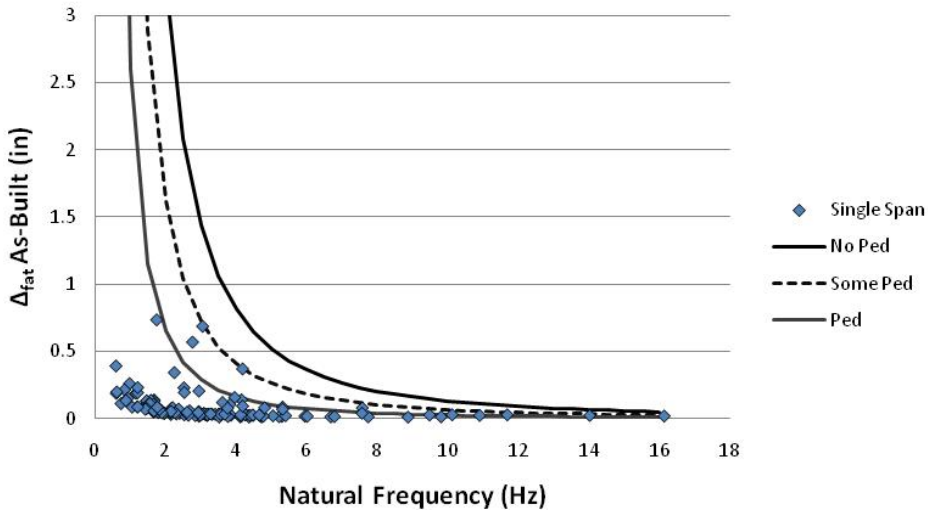


**Figure 3-8 Fatigue As-Built Deflections vs. Natural Frequencies for Simple Spans**

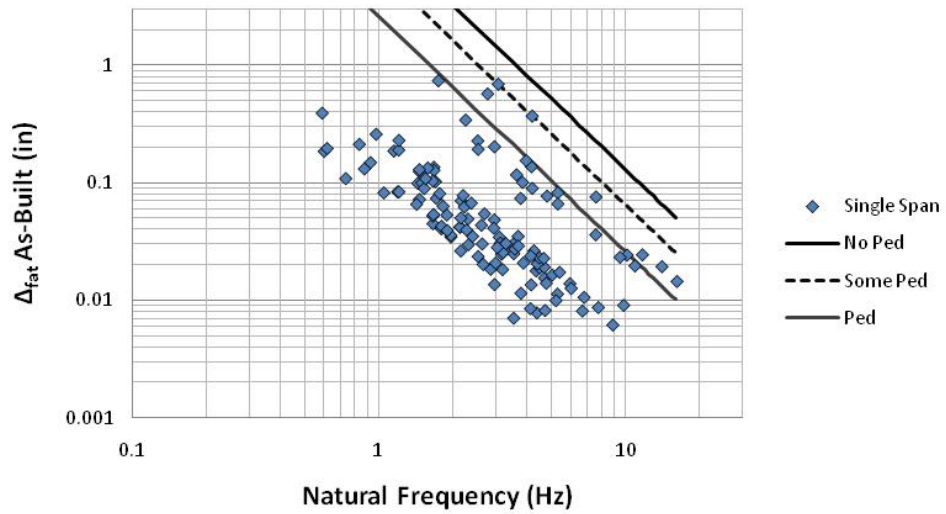


**Figure 3-9 Fatigue As-Built Deflections vs. Natural Frequencies for Simple Spans Log-Log Axis**

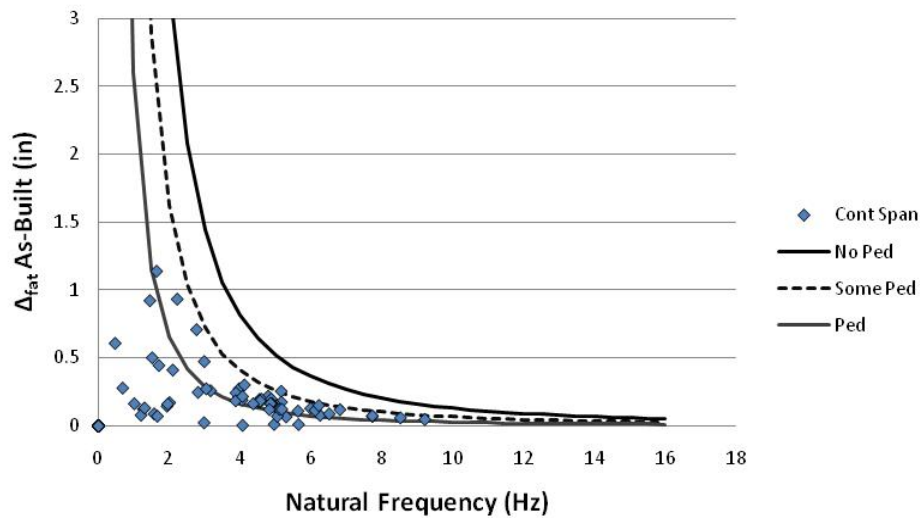


**Figure 3-10 Fatigue As-Built Deflections vs. Natural Frequencies for Continuous Spans**

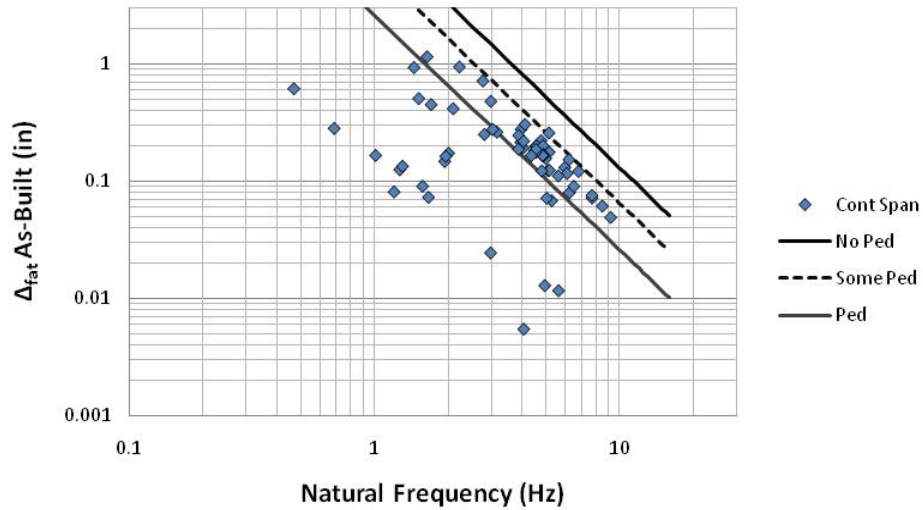


**Figure 3-11 Fatigue As-Built Deflections vs. Natural Frequencies for Continuous Spans Log-Log Axis**

These figures show that all of the bridges satisfy the criteria for bridges with no intended pedestrian use. However, several bridges violate the limit for bridges with heavy intended pedestrian use, and a few bridges violate the limit for bridges with some intended pedestrian use. All bridges pass current AASHTO Service I criteria, yet the correlated OHBC criteria indicates some of these bridges are unsatisfactory for pedestrian use. This indicates a possible inadequacy of current AASHTO Service I criteria in controlling bridge vibrations. Additionally, the figures show that the deflections for bridges with natural frequencies less than 2 Hz are far below the allowable deflection curve. This validates the method used in the previous section to fit power functions to the OHBC criteria.

### 3.4.3

### $X_{fat}$ As-Built

In order to determine if the proposed user comfort formulation successfully incorporates natural frequency and to gain a better understanding of the behavior of the X factors, the back-calculated X factors for the fatigue as-built loading,  $X_{fat}$ , are plotted compared to the span length. Additionally, the limiting X factors,  $X_{lim}$ , are plotted for the three levels of intended pedestrian use. Figure 3-12 shows the plot for simple spans, and Figure 3-13 shows the figure for continuous spans. A data point with a value greater than the limiting  $X_{lim}$  line violates that respective proposed formulation. For example, a data point with a value greater than the  $X_{lim}$  for some intended pedestrian use is unsatisfactory for a bridge with some intended pedestrian use. A given bridge structure may be acceptable for a bridge with no intended pedestrian use, but unacceptable for either some or heavy intended pedestrian use.

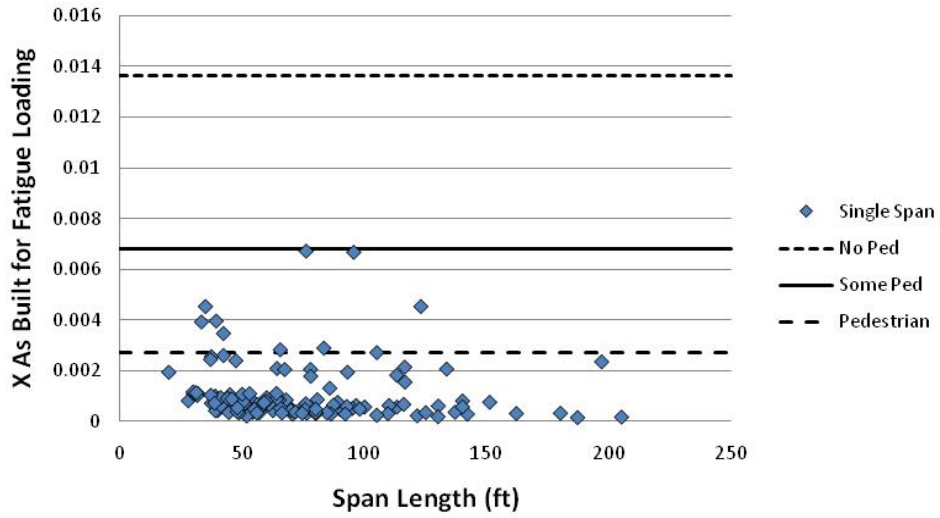


**Figure 3-12  $X_{fat As-Built}$ ,  $X_{lim}$ , vs. Span Length Simple Spans**

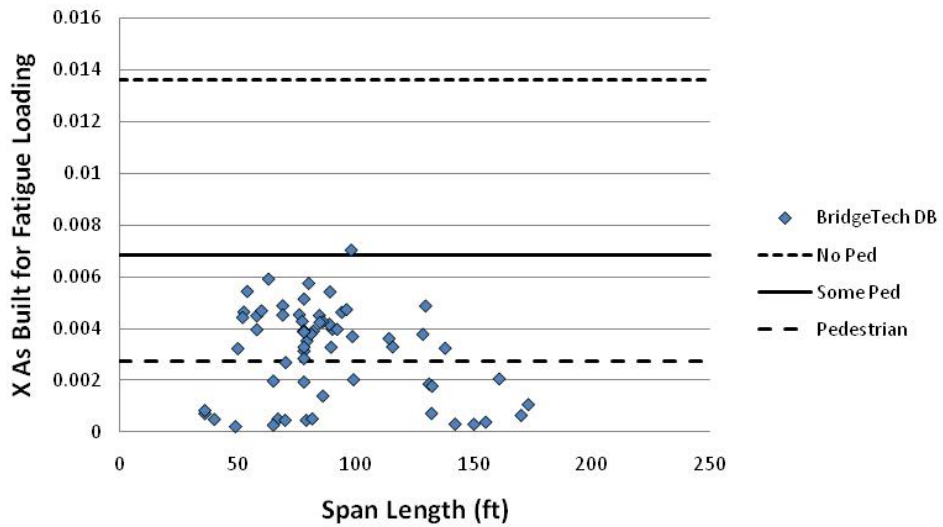


**Figure 3-13  $X_{fat As-Built}$ ,  $X_{lim}$ , vs. Span Length Continuous Spans**

These figures show that all 195 bridges within the bridge suite satisfy the proposed criteria for bridges with no intended pedestrian use. The

figures also show that several of the bridges violate the limits for both some and heavy pedestrian use. This shows the same possible inadequacy of the AASHTO Service I criteria as the deflection versus natural frequency plots in Section 3.4.2. This similar behavior shows that the proposed formulation successfully incorporates natural frequency.

### **3.4.4 Allowable Deflections**

By plotting the ratios of the fatigue as-built deflections to the allowable deflections, as per the proposed  $X_{lim}$  method, the same relations shown in Section 3.4.3 can be shown in a more linear fashion. The deflection ratios are plotted compared to span length for simple spans in Figure 3-14, and continuous spans in Figure 3-15. Each bridge has three deflection ratios, one for each level of intended pedestrian use. Any data point with a value higher than 1.0 shows a violation for that respective proposed criterion. These figures show, in a more linear sense, which bridges would fail the proposed criteria when correlated to the OHBC.

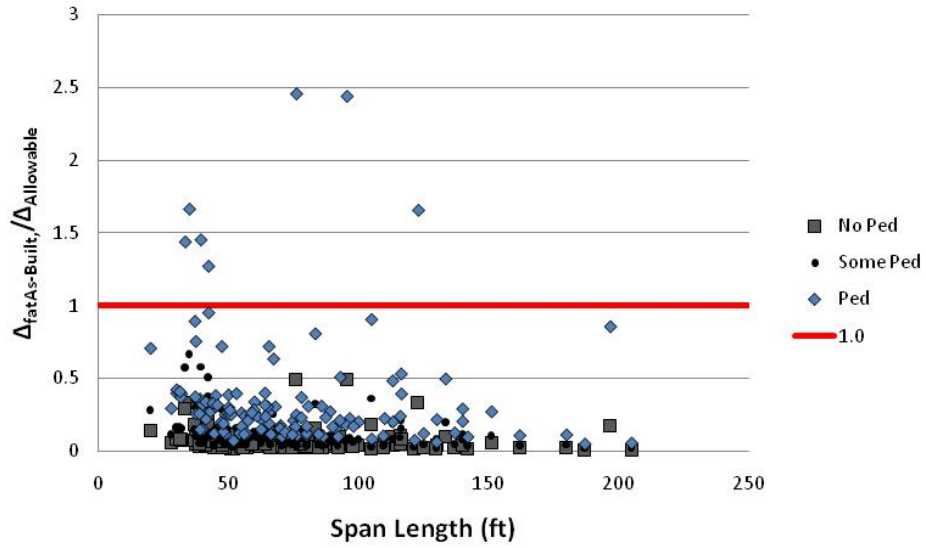


**Figure 3-14  $\Delta_{fatAs-Built}/\Delta_{Allowable}$  vs. Span Length Simple Spans**

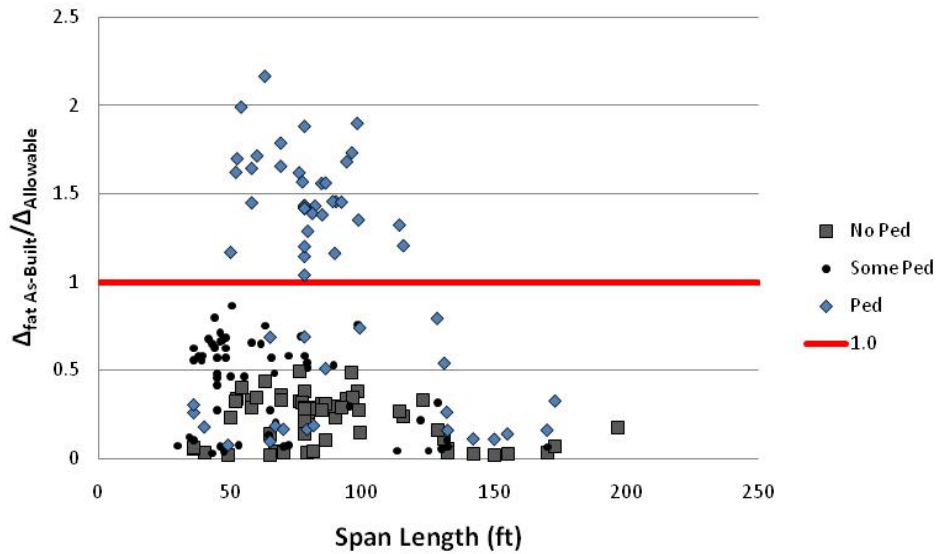


**Figure 3-15  $\Delta_{fatAs-Built}/\Delta_{Allowable}$  vs. Span Length Continuous Spans**

These figures clearly show several bridges failing the proposed criteria for heavy intended pedestrian use. This again shows a possible inadequacy in the current AASHTO criteria to control bridge vibrations.



In order to compare the current AASHTO Service I criteria to the proposed formulations, the maximum allowable deflections are compared. Since the proposed formulation uses deflections induced by the fatigue truck load and not the Service I load, the L/800 and L/1000 deflection limits are factored by the average ratio of Fatigue to Service I deflections, as in Section 3.4.2. The factored L/800 criterion is used in figures for no intended pedestrian traffic, while the factored L/1000 criterion is used for intended pedestrian traffic. The maximum allowable deflections for no intended pedestrian traffic are compared in Figure 3-16 for simple spans and Figure 3-17 for continuous spans. The maximum allowable deflections for some intended pedestrian traffic are compared in Figure 3-18 for simple spans and Figure 3-19 for continuous spans. The maximum allowable deflections for heavy intended pedestrian traffic are compared in Figure 3-20 for simple spans and Figure 3-21 for continuous spans. A data point above the Service I criteria line represents a bridge that may have a deflection larger than the current AASHTO criteria and still satisfy user comfort criteria. A data point below the line labeled Ser I means the proposed criteria would be more restrictive than current AASHTO criteria.

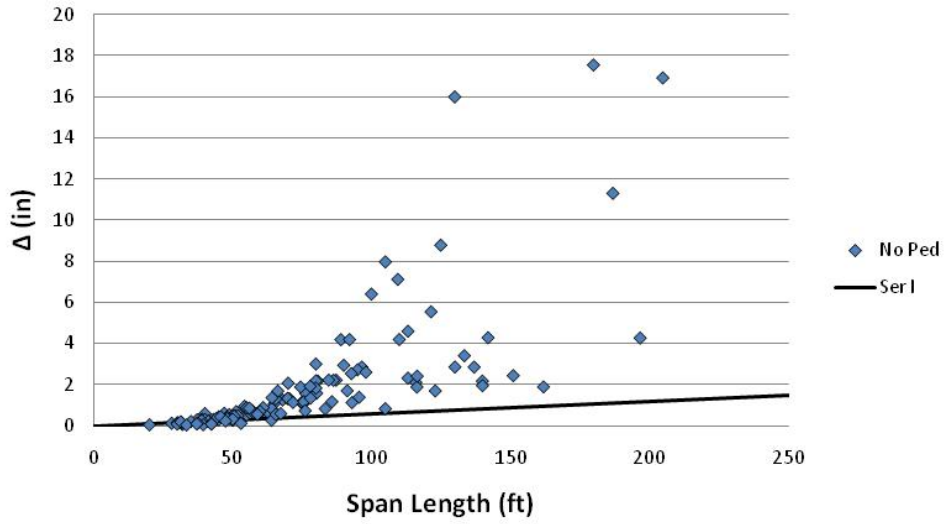


**Figure 3-16 Maximum Allowable Deflections No Intended Pedestrian Use Simple Spans**

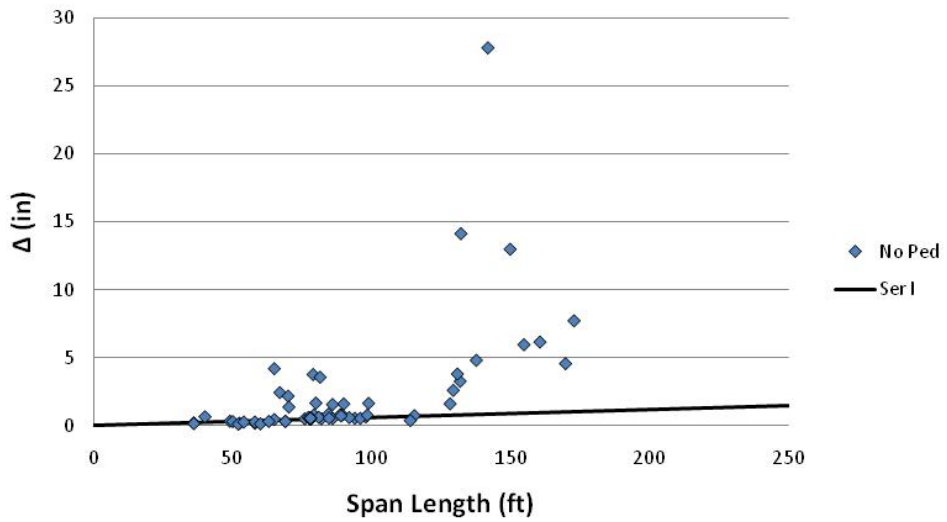


**Figure 3-17 Maximum Allowable Deflections No Intended Pedestrian Use Continuous Spans**

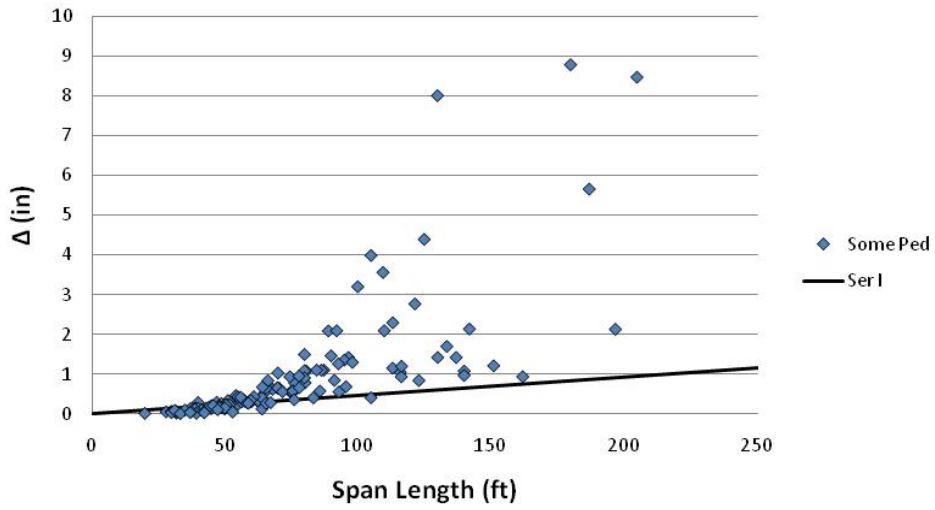


**Figure 3-18 Maximum Allowable Deflections Some Intended Pedestrian Use Simple Spans**

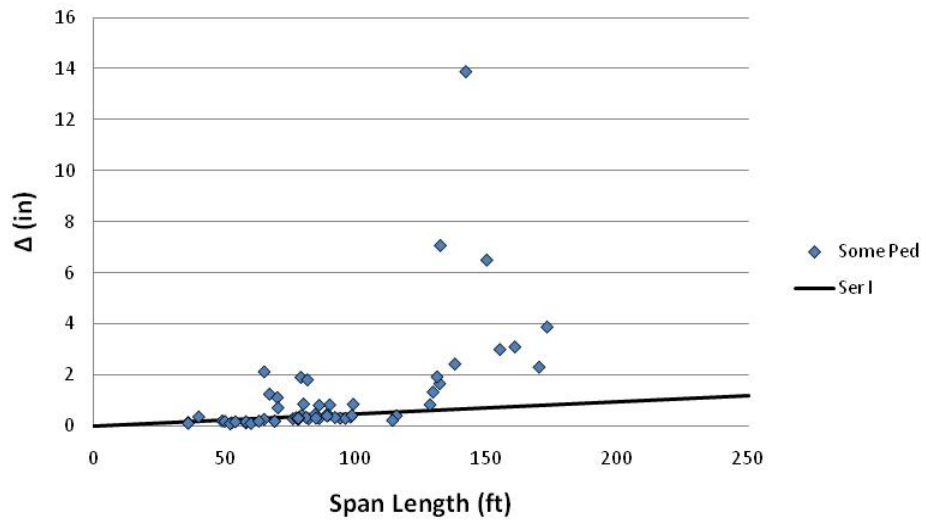


**Figure 3-19 Maximum Allowable Deflections Some Intended Pedestrian Use Continuous Spans**

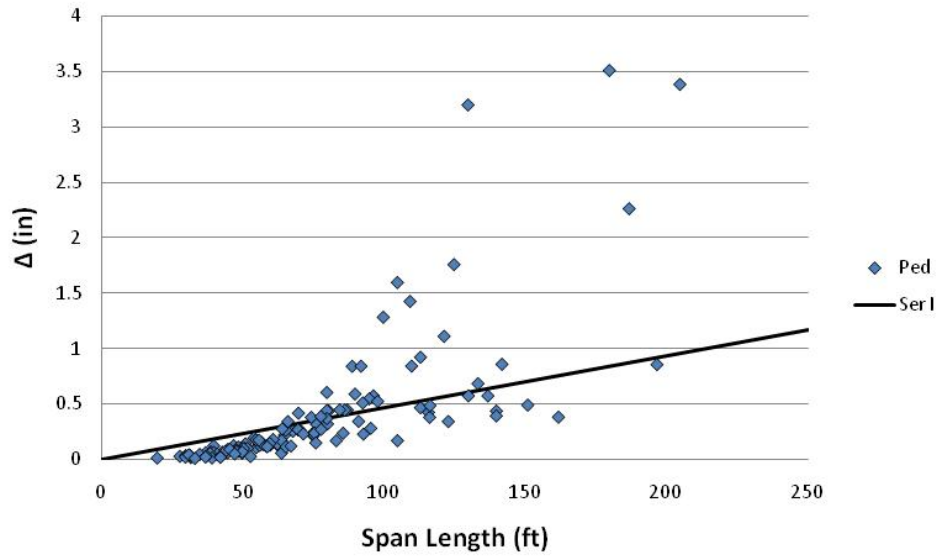


**Figure 3-20 Maximum Allowable Deflections Heavy Intended Pedestrian Use Simple Spans**

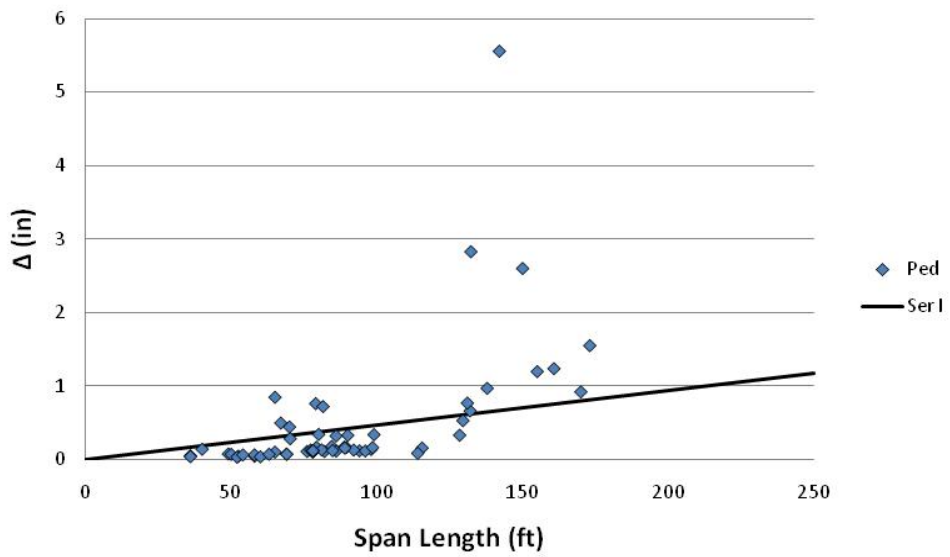


**Figure 3-21 Maximum Allowable Deflections Heavy Intended Pedestrian Use Continuous Spans**

Results from these figures suggest several conclusions about the maximum allowable deflections based on the  $X_{lim}$  method. First is that there is a wide range of allowable deflections ranging from under 1 inch to just under 30 inches for bridges with no intended pedestrian traffic. A deflection of 30 inches is a large deflection. Not surprisingly, these larger allowable deflections occur for bridges with longer spans. These particular longer spanned bridges have a lower natural frequency. These properties result in a lower acceleration for a given deflection compared to a stiffer, shorter bridge. This relation is clearly shown in the natural frequency vs. maximum allowable deflection plots in Section 3.4.2. While this high of a deflection may provoke an initial alarming result, other limit states would prevent this large deflection from occurring. The continuous span bridge with the high allowable deflection still has an as-built deflection below the AASHTO limit. The large allowable deflection indicates that user comfort is unlikely to be a controlling factor in design for that particular bridge.

The data displayed in the above figures allows for a comparison between the current AASHTO Service I method and the proposed  $X_{lim}$  formulation. For bridges with no intended pedestrian use, the proposed  $X_{lim}$  tends to yield maximum allowable deflections greater than the current AASHTO Service I maximum allowable deflections. This suggests that for bridges with no intended pedestrian use, the  $X_{lim}$  method is less conservative

and therefore more economical. For bridges with some intended pedestrian use, most of the bridges have a higher allowable deflection with the  $X_{lim}$  method; however, for some of the bridges the proposed  $X_{lim}$  formulation yields smaller maximum allowable deflection than the Service I criteria. This mix is further demonstrated for bridges with heavy intended pedestrian use in which most of the bridges have a lower maximum allowable deflection with the  $X_{lim}$  method than the Service I limiting deflection. This suggests that the current AASHTO Service I limits may be inadequate in preventing user discomfort for bridges with intended pedestrian use.

The results shown in this section are only for the bridges with the as-built load. These results do not necessarily demonstrate the response when a bridge is at its optimal design limit state. Most of the bridges in the database are oversized. Thus, the responses of concern are lower than those that would be present with a bridge performing at an optimal design state. In order to model this response, a method is required to optimize a bridge.

### **3.5 Bridge Optimization**

In order to model the response of a bridge at an optimal design limit state, an optimization process must be derived. The amount of overdesign can be represented by the rating factor. For instance, with a rating factor of 1.50, the bridge can withstand 50% more truck loading before reaching the optimized design limit. In this way rating factors using the 2002 AASHTO

LRFD Design Specifications can be used to alter the load so that the bridge response represents the response at the optimal design limit state. These bridges with the factored loads will be referred to as optimized bridges in this research effort.

### 3.5.1 Derivation of Bridge Optimization

This section derives the bridge optimization process for the AASHTO LRFD 2002 Design Specification limit states of Strength I, Service II, and Service I.

#### 3.5.1.1 Strength I

The equation for the Strength I rating factor for the bridge as-built is given by Equation 3-34 as:

$$RF_{S_{I1}} = \frac{S_{bn}}{1.75M_{LL+IM}} \cdot \left( \phi_f F_{no} - \frac{1.25M_{DC1}}{S_{bst1}} - \frac{1.25M_{DC2}}{S_{BEM}} - \frac{1.5M_{DW}}{S_{BEM}} \right)$$

(Eqn 3-34)

The equation for the Strength I rating factor for the optimized bridge by changing the load is given by Equation 3-35 below.

$$RF_{S_{I1Opt}} = \frac{S_{bn}}{1.75M_{LL+IMOpt}} \cdot \left( \phi_f F_{no} - \frac{1.25M_{DC1}}{S_{bst1}} - \frac{1.25M_{DC2}}{S_{BEM}} - \frac{1.5M_{DW}}{S_{BEM}} \right)$$

(Eqn 3-35)

Since the bridge cross section does not change, the section modulus and dead load moment components do not change. The optimized rating factor is set equal to one and then Equation 3-34 is divided by Equation 3-35 yielding:

$$\phi_f F_{no} = \frac{1.25M_{DC1}}{S_{nom}} - \frac{1.25M_{DC2}}{S_{nom}} - 1.5M_{DW}$$

$$\phi_f F_{no} = \frac{1.25M_{DC1}}{S_{nom}} - \frac{1.25M_{DC2}}{S_{nom}} - 1.5M_{DW}$$

$$RF_{total} = \frac{M_{LL+IMOpt}}{M_{LL+IM}}$$

(Eqn 3-36)

### 3.5.1.2 Service II

Equation 3-37 gives the rating factor equation for the AASHTO LRFD Service II limit state for the bridge as-built.

$$RF_{SerII} = \frac{S_{bn}}{1.3 \cdot M_{LL+IM}} \left( 0.95 \cdot \phi \cdot F_{no} - \frac{M_{DC1}}{S_{bn}} - \frac{M_{DC2}}{S_{bn}} - \frac{M_{DW}}{S_{bn}} \right)$$

(Eqn 3-37)

Equation 4-38 gives the equation for the optimized rating factor.

$$RF_{SerIIOpt} = \frac{S_{bn}}{1.3 \cdot M_{LL+IMOpt}} \left( 0.95 \cdot \phi \cdot F_{no} - \frac{M_{DC1}}{S_{bn}} - \frac{M_{DC2}}{S_{bn}} - \frac{M_{DW}}{S_{bn}} \right)$$

(Eqn 3-38)



The optimized rating factor is set equal to one and dividing Equation 3-37 by Equation 3-38 yields.

$$\frac{RF_{Service}}{1} = \frac{\frac{S_{Bn}}{1.3 \cdot M_{LL+IM}} \left( 0.95 \cdot \phi \cdot F_{nc} - \frac{M_{DC1}}{S_{bst1}} - \frac{M_{DC2}}{S_{Bn}} - \frac{M_{DW}}{S_{Bn}} \right)}{\frac{S_{Bn}}{1.3 \cdot M_{LL+IMOpt}} \left( 0.95 \cdot \phi \cdot F_{nc} - \frac{M_{DC1}}{S_{bst1}} - \frac{M_{DC2}}{S_{Bn}} - \frac{M_{DW}}{S_{Bn}} \right)}$$

$$\frac{RF_{Service}}{1} = \frac{\frac{S_{Bn}}{1.3 \cdot M_{LL+IM}} \left( 0.95 \cdot \phi \cdot F_{nc} - \frac{M_{DC1}}{S_{bst1}} - \frac{M_{DC2}}{S_{Bn}} - \frac{M_{DW}}{S_{Bn}} \right)}{\frac{S_{Bn}}{1.3 \cdot M_{LL+IMOpt}} \left( 0.95 \cdot \phi \cdot F_{nc} - \frac{M_{DC1}}{S_{bst1}} - \frac{M_{DC2}}{S_{Bn}} - \frac{M_{DW}}{S_{Bn}} \right)}$$

$$RF_{Service} = \frac{M_{LL+IMOpt}}{M_{LL+IM}}$$

(Eqn 3-39)

### 3.5.1.3 Service I

Equation 3-40 gives the definition of the AASHTO LRFD Service I limit state rating factor.

$$RF_{Service} = \frac{\Delta_{Limit}}{\Delta_{Service}}$$

(Eqn 3-40)

Equation 3-41 gives the optimized Service I rating Factor below.

$$RF_{ServiceOpt} = \frac{\Delta_{Limit}}{\Delta_{ServiceOpt}}$$

(Eqn 3-41)

The limiting deflection remains the same as the span lengths do not change, however the Service I deflection will change. The equation for Service I deflection is shown below in Equation 3-42.

$$\Delta_{\text{ServI}} = \frac{M_{LL+IN} \cdot f(x, L_{\text{span}})}{EI}$$

(Eqn 3-42)

where

$f(x, L_{\text{span}})$  = a function in terms of bridge location (x) and span length ( $L_{\text{span}}$ )

This function is the same for both the bridge as-built and the optimized bridge when the optimization process only changes the loading applied to the bridge. Therefore the optimized deflection is given by Equation 3-43 below.

$$\Delta_{\text{ServIOpt}} = \frac{M_{LL+IMOpc} \cdot f(x, L_{\text{span}})}{EI}$$

(Eqn 3-43)

Substituting the equation for the Service I deflection, Equation 3-42, into the as-built rating factor equation, Equation 3-40, yields:

$$RF_{\text{ServI}} = \frac{\Delta_{\text{Limit}}}{\frac{M_{LL+IN} \cdot f(x, L_{\text{span}})}{EI}}$$

(Eqn 3-44)

In a similar manner substituting the optimized Service I deflection, Equation 3-43, into the optimized rating factor equation, Equation 3-41, yields:

$$RF_{ServIopt} = \frac{\Delta_{limIt}}{M_{LL+IMOpt} \cdot f(X, L_{span}) / BI}$$

(Eqn 3-45)

The as-built rating factor, Equation 3-44, is then divided by the optimized rating factor, Equation 4-45, with the optimized Service I rating factor set equal to one which simplifies and results in Equation 3-46.

$$\frac{RF_{ServI}}{1} = \frac{\frac{\Delta_{limIt}}{M_{LL+IM} \cdot f(X, L_{span}) / BI}}{\frac{\Delta_{limIt}}{M_{LL+IMOpt} \cdot f(X, L_{span}) / BI}}$$

$$\frac{RF_{ServI}}{1} = \frac{\frac{\Delta_{limIt}}{M_{LL+IM} \cdot f(X, L_{span}) / BI}}{\frac{\Delta_{limIt}}{M_{LL+IMOpt} \cdot f(X, L_{span}) / BI}}$$

$$RF_{ServI} = \frac{M_{LL+IMOpt}}{M_{LL+IM}}$$

(Eqn 3-46)

### 3.5.1.4 Optimized Rating Factor

The relationship between the rating factor, live load moment as-built, and live load moment optimized for the Strength I, Service II, and Service I limit states all follow the form shown in Equation 3-47.

$$RF_j = \frac{M_{LL+IMOPT}}{M_{LL+IN}}$$

(Eqn 3-47)

where

j = limit state for optimization (Strength I, Service II, Service I)

Using this equation, the governing rating factor is the minimum rating factor of the three limit states (Strength I, Service II, Service I). This minimum rating factor is used in calculating the optimized deflections and X factors which is detailed in following section.

### **3.5.2 Calculating Optimized Deflections and X factors**

This section derives the calculation for optimized deflections and X factors, and then proceeds to use Missouri A6101 for sample calculations of optimized deflections and X factors.

#### **3.5.2.1 Derivation**

Dividing the as-built deflection by the optimized deflection results in the following relation between the ratio of as-built to optimized deflections in terms of the live load moments yields:

$$\frac{\Delta_{iAs-Built}}{\Delta_{iOpt}} = \frac{\frac{M_{LL+IM} \cdot f(X, L_{span})}{EI}}{\frac{M_{LL+IMOpt} \cdot f(X, L_{span})}{EI}}$$

$$\frac{\Delta_{iAs-Built}}{\Delta_{iOpt}} = \frac{\frac{M_{LL+IM} \cdot f(X, L_{span})}{EI}}{\frac{M_{LL+IMOpt} \cdot f(X, L_{span})}{EI}}$$

$$\frac{\Delta_{iAs-Built}}{\Delta_{iOpt}} = \frac{M_{LL+IM}}{M_{LL+IMOpt}}$$

This rearranged gives Equation 3-48, which defines the optimized deflection.

$$\Delta_{iOpt} = \frac{M_{LL+IMOpt}}{M_{LL+IM}} \Delta_{iAs-Built}$$

(Eqn 3-48)

The controlling rating factor, Equation 3-47, is then substituted into the definition of the optimized deflection, Equation 3-48, to yield:

$$\Delta_{iOpt} = RF_{CTRL} \cdot \Delta_{iAs-Built}$$

(Eqn 3-49)

Where i denotes the load applied to the bridge. Optimized Service I deflections can be calculated as:

$$\Delta_{ServiceOpt} = RF_{CTRL} \cdot \Delta_{Service}$$

(Eqn 3-50)

Optimized fatigue truck load deflections can be calculated as:

$$\Delta_{fatOpt} = RF_{CTRL} \cdot \Delta_{fat}$$

(Eqn 3-51)

Equation 3-17 gives the definition for the X factor which is shown below for the optimized bridge.

$$X_{iOpt} = \frac{\Delta_{iOpt} \cdot \lambda^4 \cdot E \cdot I_B}{W \cdot L^4}$$

Substituting Equation 3-49 into the X factor definition yields the following:

$$X_{iOpt} = \frac{RF_{CTRL} \Delta_i \cdot \lambda^4 \cdot E \cdot I_B}{W \cdot L^4}$$

where i denotes the loading type of either fatigue truck loading or Service I loading. Substituting the definition of X for the bridge as-built, Equation 3-17, yields:

$$X_{iOpt} = RF_{CTRL} \cdot X_i$$

(Eqn 3-52)

The optimized X factors for Service I and fatigue truck loading are given in Equations 3-52 and 3-53 below.

$$X_{ServiceOpt} = RF_{CTRL} \cdot X_{Service}$$

(Eqn 3-53)

$$X_{fatopt} = RF_{CTRL} \cdot X_{fat}$$

(Eqn 3-54)

### 3.5.2.2 Sample Calculations for Missouri Bridge A6101

This section uses Missouri Bridge A6101 to demonstrate the previously derived optimization calculation procedures used within this research effort. The controlling 2002 AASHTO LRFD design bridge specification factor of safety is the Strength I rating factor of 0.934.

#### 3.5.2.2.1 Calculating Optimized Deflections

Equation 3-50 is applied and used to calculate the optimized Service I deflection while Equation 3-51 is applied to calculate the optimized fatigue load deflection.

$$\Delta_{serviOpt} = RF_{CTRL} \cdot \Delta_{servi}$$

$$\Delta_{serviOpt} = 0.934 \cdot 1.324in$$

$$\Delta_{serviOpt} = 1.237in$$

$$\Delta_{fatOpt} = RF_{CTRL} \cdot \Delta_{fat}$$

$$\Delta_{fatOpt} = 0.934 \cdot 0.549in$$

$$\Delta_{fatOpt} = 0.513in$$

#### 3.5.2.2.2 Calculating Optimized X Factors

Equation 3-53 is applied to calculate the optimized Service I deflection X factor and Equation 3-54 is applied to calculate the optimized fatigue deflection X factor.

$$X_{SerIopt} = RF_{CTEL} \cdot X_{SerI}$$

$$X_{SerIopt} = 0.934 \cdot 0.0038$$

$$X_{SerIopt} = 0.0035$$

$$X_{fatopt} = RF_{CTEL} \cdot X_{fat}$$

$$X_{fatopt} = 0.934 \cdot 0.0016$$

$$X_{fatopt} = 0.0015$$

These same calculations were performed for each of the 195 bridges within the bridge suite. The results of these calculations are shown in the next section.

### 3.5.3 Results for Bridges with Optimized Loading

This section shows and analyzes the results from the calculations performed in the previous section when applied to each bridge in the bridge suite.

#### 3.5.3.1 Optimized Service I Deflections

In order to gain a better understanding of the behavior of the bridges at the optimal design limit state with regards to the current AASHTO



deflection criteria, the Service I optimized deflections are plotted against the span length for simple spans in Figure 3-22 and continuous spans in Figure 3-21. The figures also show the plotted allowable deflection limits for the current AASHTO Service I criteria.

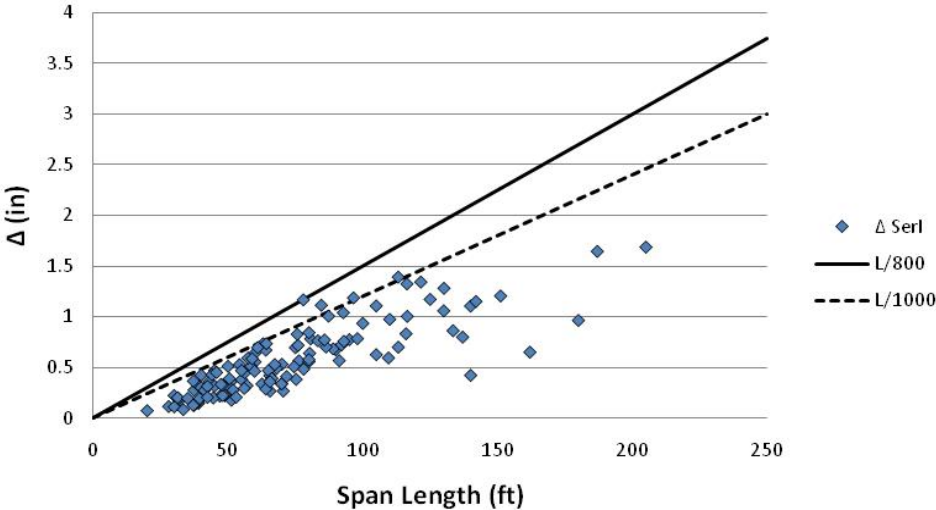


**Figure 3-22 Optimized Service I Deflections vs. Span Length Simple Spans**

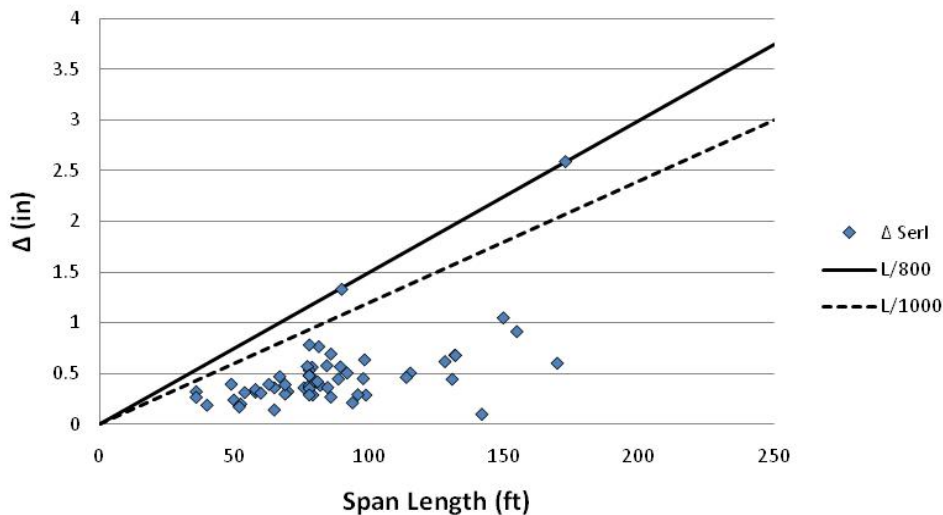


**Figure 3-23 Optimized Service I Deflection vs. Span Length Continuous Spans**

The figures show that none of the optimized bridges exceed the non-pedestrian AASHTO Service I criteria.

### 3.5.3.2 Optimized Fatigue Deflections

In order to gain a better understanding of the behavior of the bridges at the optimal design limit state with respect to fatigue deflections, the optimized fatigue deflections are plotted compared to span length. Since the L/800 and L/1000 deflection limits are correlated to the Service I deflections, it is not appropriate to compare the fatigue deflection to these limits. Instead the deflection criterion is multiplied by the average of the ratio of fatigue to Service I deflections. The fatigue optimized deflections are plotted against

span length for simple spans in Figure 3-24 and continuous spans in Figure 3-25.

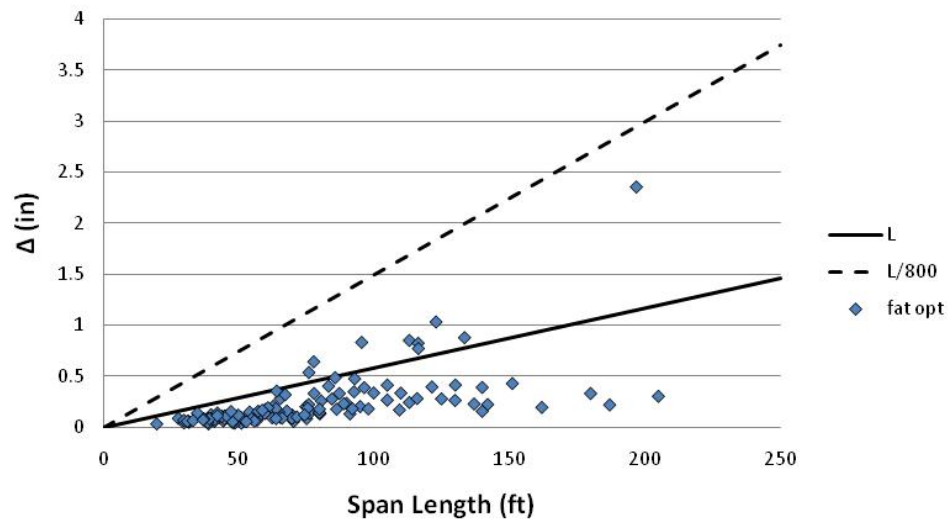


**Figure 3-24 Optimized Fatigue Deflections vs. Span Length Simple Spans**

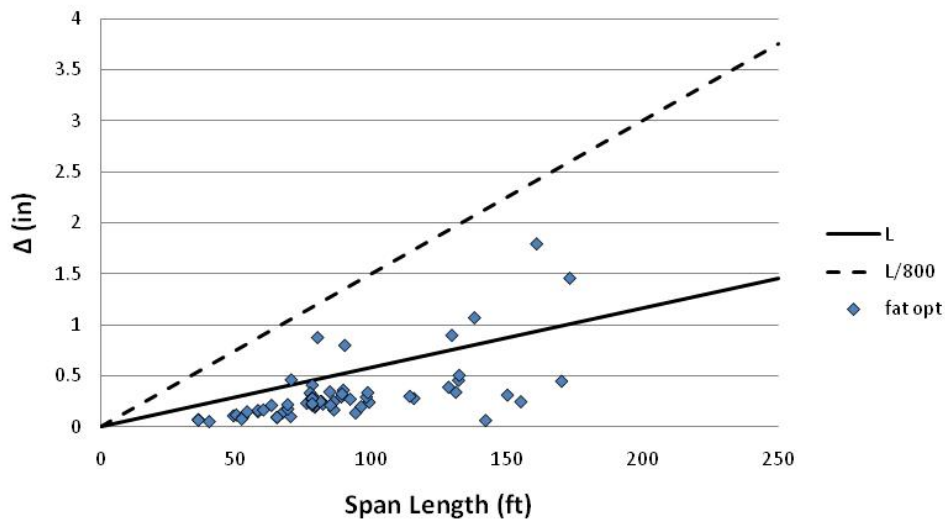


**Figure 3-25 Optimized Fatigue Deflections vs. Span Length Continuous Spans**

These figures show similar behavior as the previous Service I deflection figures in Section 3.5.3.1. All of the bridges meet the criteria for the no pedestrian limit, while the majority of bridges meet the pedestrian limit.

The optimized fatigue deflections are plotted versus the bridge natural frequencies in order to analyze this relation. Figure 3-26 shows the optimized fatigue deflections versus natural frequency for simple span bridges and Figure 3-27 shows the same relation on a log-log scale. Figure 3-28 shows the optimized fatigue deflections versus natural frequency for continuous spans, and Figure 3-29 shows the same relation with a log-log axis. These figures also include the approximate functions relating maximum deflection to natural frequency, Equations 3-24 through 3-26. A

data point above this line indicates a violation of the criteria for a particular level of intended pedestrian use.

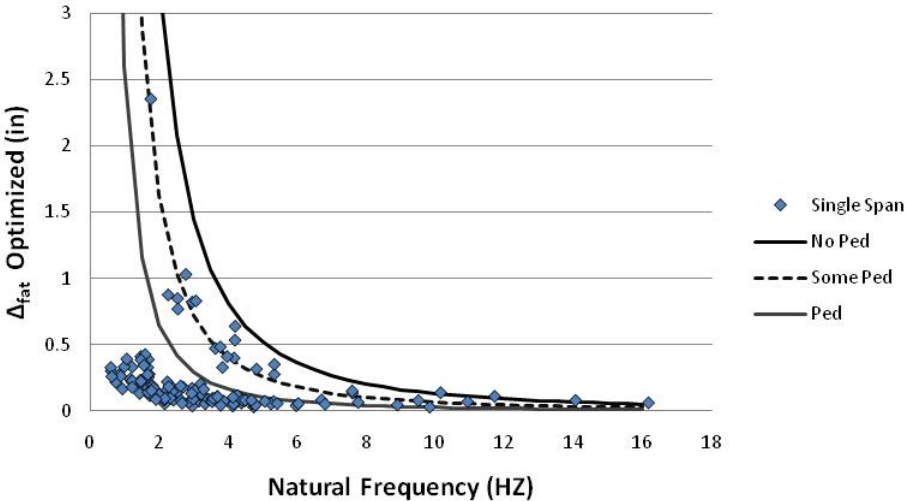


**Figure 3-26 Optimized Fatigue Deflections vs. Natural Frequency for Simple Spans**

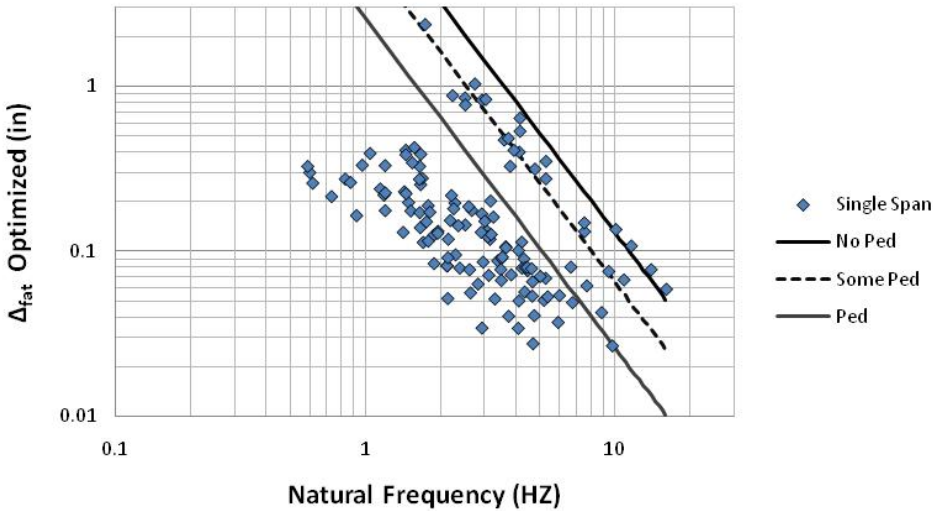


**Figure 3-27 Optimized Fatigue Deflections vs. Natural Frequency for Simple Spans Log-Log Axis**

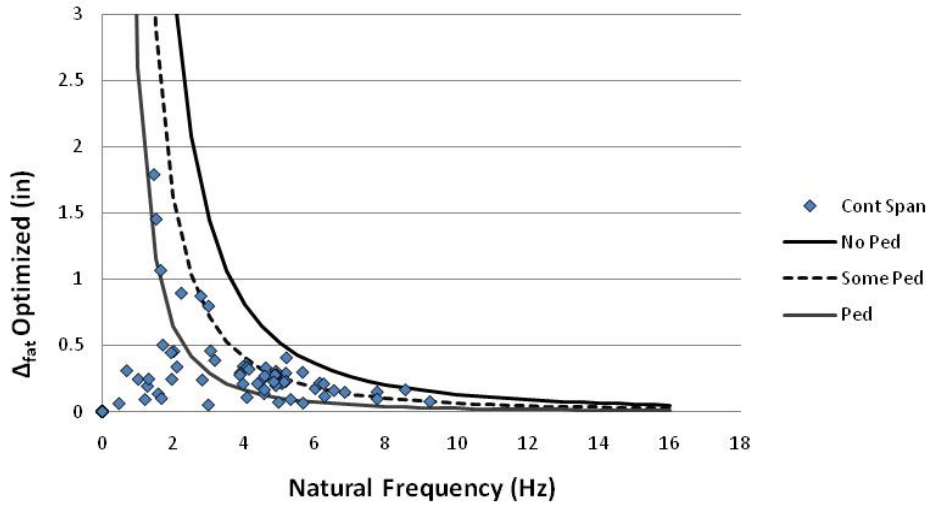


**Figure 3-28 Optimized Fatigue Deflections vs. Natural Frequency for Continuous Spans**

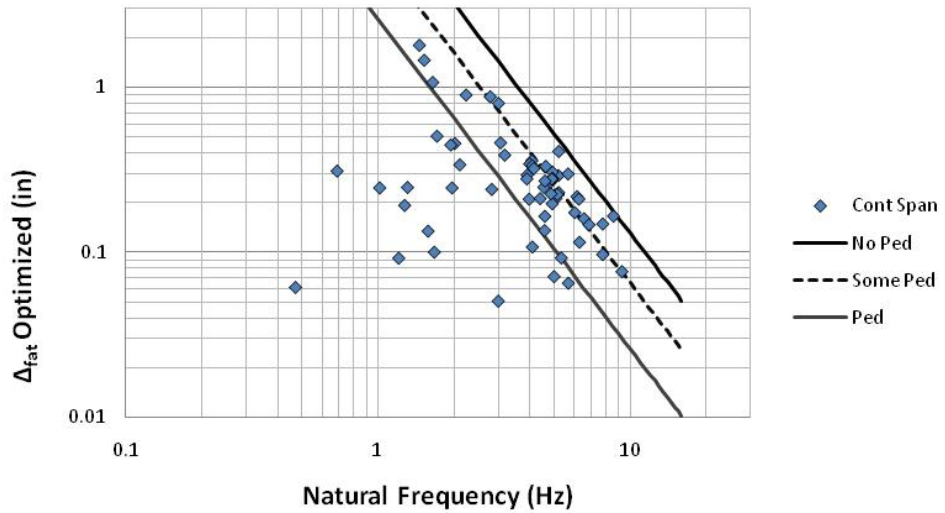


**Figure 3-29 Optimized Fatigue Deflections vs. Natural Frequency for Continuous Spans Log-Log Axis**

While all of the optimized bridges were adequate for user comfort using the current AASHTO Service I criteria for no intended pedestrian use, several optimized bridges violate even the most liberal proposed user comfort criteria. Additionally, the majority of optimized bridges successfully met the pedestrian Service I criteria; however, a large number of bridges violate the proposed criteria for some intended pedestrian use and heavy intended pedestrian use. This is a strong indication that current AASHTO Service I criteria may be insufficient to control bridge vibrations.

### **3.5.3.3 Optimized Fatigue X factors and $X_{lim}$**

In order to gain a better understanding of the behavior of the bridge response at the optimal design limit, the back-calculated X factors for the fatigue optimized loading,  $X_{fatOpt}$ , are plotted compared to the span length. Additionally, the limiting X factors,  $X_{lim}$ , are plotted for the three levels of intended pedestrian use. Figure 3-30 shows the plot for simple spans, and Figure 3-31 shows the figure for continuous spans. A data point above the limiting  $X_{lim}$  line violates that respective proposed formulation. For example, a data point with a value higher than the  $X_{lim}$  for some intended pedestrian use is unsatisfactory for a bridge with some intended pedestrian use. A given bridge structure may be acceptable for a bridge with no intended pedestrian use, but unacceptable for either some or heavy intended pedestrian use.

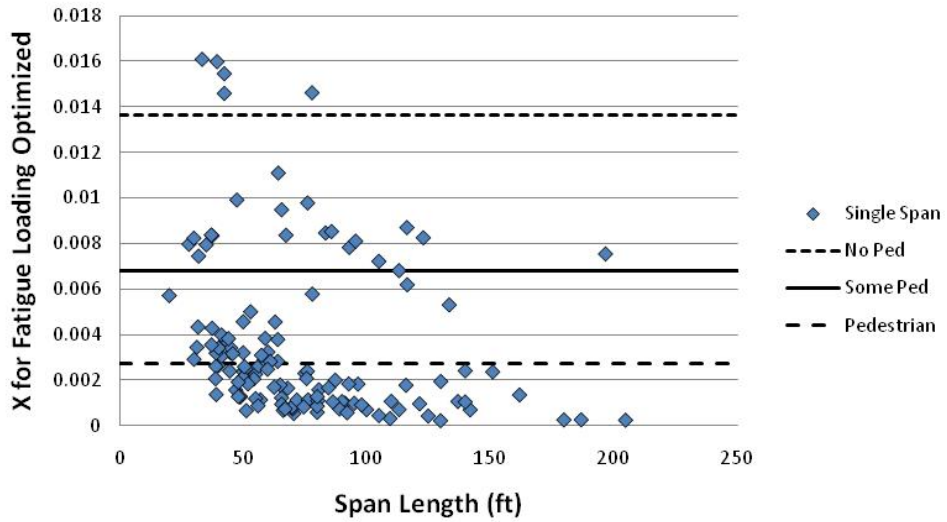


**Figure 3-30  $X_{fat\ Optimized}$ ,  $X_{lim}$ , vs. Span Length Simple Spans**

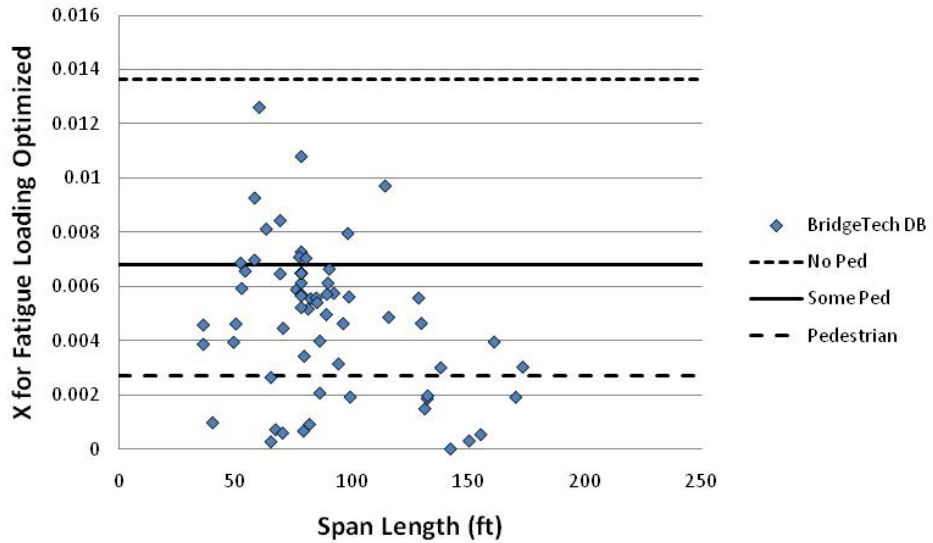


**Figure 3-31  $X_{fat\ Optimized}$ ,  $X_{lim}$ , vs. Span Length Continuous Spans**

These figures show that five optimized bridges violate the most liberal of the proposed criteria for no intended pedestrian use. A majority of



the optimized bridges violate the proposed criteria for either some or heavy intended pedestrian use. Each of the optimized bridges met the current AASHTO Service I criteria for no intended pedestrian use, and the majority met the Service I criteria for intended pedestrian use. This strongly indicates a possible inadequacy in the current AASHTO Service I criteria to control excess bridge vibration. This possible inadequacy is even more pronounced in bridges with heavy intended pedestrian use. A significant number of bridges in the bridge suite violate this most conservative limit when the bridge is optimized for current AASHTO design limit states.

#### **3.5.3.4 Optimized Deflection Ratios**

By plotting the ratio of optimized fatigue deflection to the maximum allowable deflection, the relations showed in the previous section can be observed in a more linear fashion. The deflection ratios are plotted compared to span length for simple spans in Figure 3-32, and Figure 3-33 shows the deflection ratios versus span length for continuous spans. Each bridge has three deflection ratios, one for each level of intended pedestrian use. Any data point with a value higher than 1.0 shows a violation for that respective proposed criterion. These figures show, in a more linear sense, which optimized bridges would fail the proposed criteria when correlated to the OHBC.

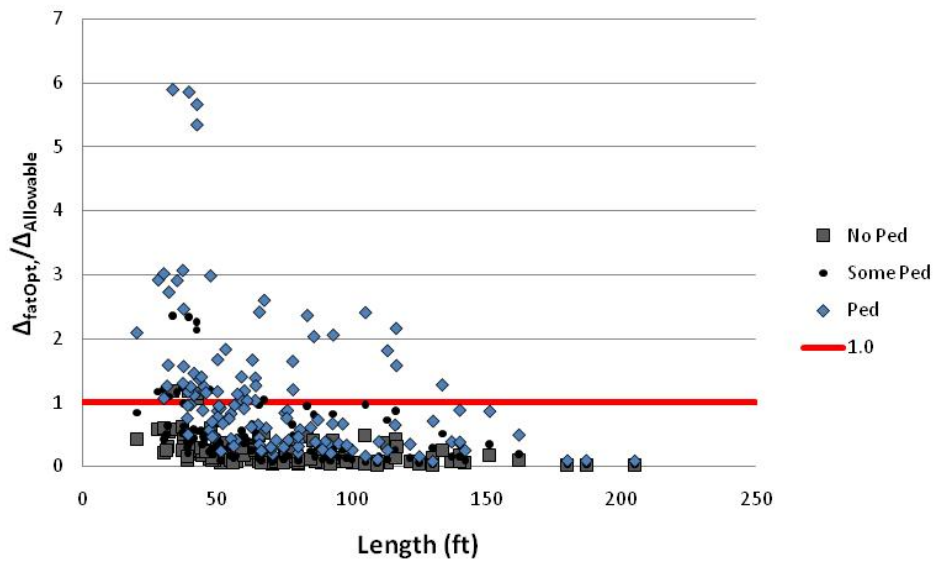


Figure 3-32  $\Delta_{fatOptimized}/\Delta_{Allowable}$  vs. Span Length Simple Spans

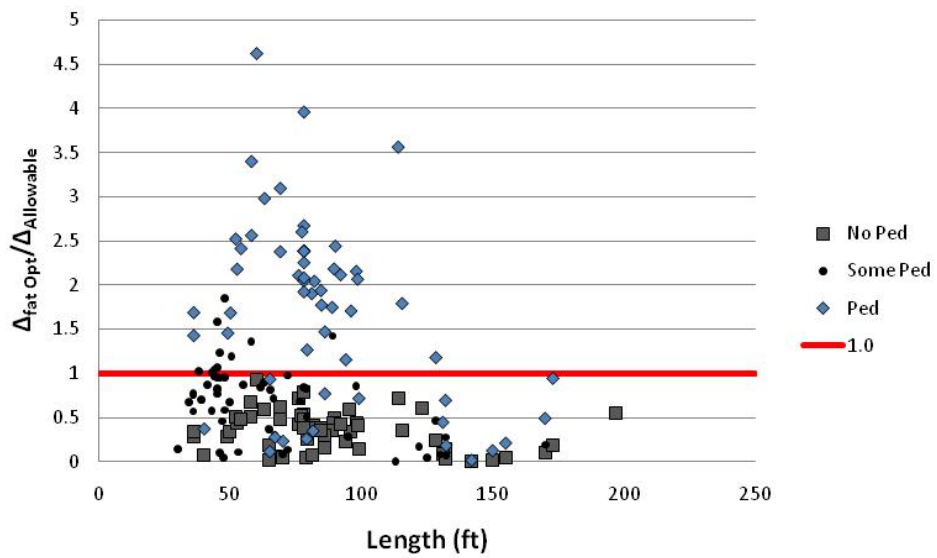


Figure 3-33  $\Delta_{fatOptimized}/\Delta_{Allowable}$  vs. Span Length Continuous Spans

These graphs clearly show the large number of optimized bridges that violate the proposed criteria for some and heavy intended pedestrian use. It also shows several bridges violating the most liberal of the proposed criteria for no intended pedestrian use. These graphs show that same indication as the figures in Section 3.5.3.3 that the current AASHTO Service I criteria may be inadequate in controlling excess bridge vibrations and, therefore, inadequate in controlling user comfort.

It should be noted that these observations are based on a rough correlation of the proposed method to the OHBC natural frequency limits. There may be large differences between the OHBC truck loading and static deflections and the AASHTO fatigue truck with dynamic deflections that would skew the data. Additionally, it is unknown whether the OHBC is overly conservative, overly liberal, or neither. It is reiterated that future research is required in order to obtain the final calibrated values for  $X_{lim}$ .

### **3.6 Summary**

This chapter derived a proposed user comfort formulation using a simple dynamic pluck test. From this pluck test, a dynamic property of the bridge was obtained. The proposed criterion, while based on the dynamic property of the natural frequency, remains in mechanics terms familiar to the typical bridge engineer. While the formulation is proposed, the final design limits ( $X_{lim}$ ) require additional research for final calibration. Missouri

Bridge A6101 was then used to demonstrate the calculation methods used within this research effort on each bridge within the suite. The results of these calculations were analyzed and discussed; however, these results do not represent the optimized bridge response. The optimization process necessary to model the optimized response is derived, and Missouri Bridge A6101 is used to demonstrate the optimization process that was applied to each bridge in the suite. The results of the optimization calculations are shown and discussed. The results indicate that the current AASHTO Service I criteria may be inadequate in controlling excess bridge vibrations and, therefore, user comfort. The results also indicate that the proposed user comfort formulation is a viable method warranting further development.

## **Chapter 4 Stress and Strain in the Concrete Slab**

### **4.1 Introduction**

A second perceived reason for enforcing the AASHTO Service I deflection limit is to prevent structural deterioration, namely cracking in the concrete slab. However, previous research studies have found no significant correlation between girder flexibility and deck deterioration (ASCE, 1958; Wright and Walker, 1971; and Goodpasture and Goodwin, 1971). Other factors such as temperature, curing conditions, casting procedures, and wind are known to contribute to deck deterioration (Wu 2003).

This research proposes a direct concrete deck performance check to prevent flexural deck cracking deterioration. The objective is to limit concrete deck strain directly when subject to the maximum expected moment demand. The maximum expected moment is the negative pier moments in continuous spans using the AASHTO LRFD Service II loading.

This chapter details the procedure used to calculate the stress and strain in the concrete deck. The procedure is applied to the bridges within the database with continuous multiple spans. The strains and stresses are compared to the Service I deflection limits and any observed trends and correlations are discussed.

## 4.2 Method for Calculating Stress and Strain in the Concrete Deck

This section details the procedure for determining stresses and strains in the concrete deck. Mechanics of materials gives the following relation between stress and moment and section modulus for a straight beam with small deflections.

$$\sigma = \frac{M}{S}$$

(Eqn 4-1)

Since deck deterioration is a serious concern and reduces the structural integrity of the bridge, the moment used should be from the largest expected load. In the current AASHTO LRFD design specifications, this largest expected load is the Service II load. The peak negative moment will be at the interior piers of the bridge. Equation 4-2 calculates this moment.

$$M_{SerII} = DF_M \cdot M_{SerII}^{single\ lane}$$

(Eqn 4-2)

where

$M_{SerII}$  = distributed peak negative moment at the pier from Service II loads,

$DF_M$  = distribution factor for moment, and

$M_{\text{SerII Single\_Gird}}$  = peak negative moment at the pier from Service II loads on a single girder.

This moment value is the moment from the entire Service II loading applied to a single girder. The distribution factor must be applied in order to yield the actual distributed moment acting in the girder.

The equation used for calculating stress thus becomes:

$$\sigma_{\text{deck}} = \frac{M_{\text{SerII}}}{S_{\text{deck}}}$$

(Eqn 4-3)

where

$\sigma_{\text{deck}}$  = stress in the concrete deck, and

$S_{\text{deck}}$  = section modulus for top of concrete deck, short term composite.

The section modulus is the section modulus for the top of the slab assuming short-term transformed properties. Even if the girder is designed noncomposite over the piers, at Service II loads, the girder will respond compositely. The section modulus was part of the given data in the bridge suite.

Hooke's law gives the equation used for relating strain to stress.

$$\epsilon_{\text{deck}} = \frac{\sigma_{\text{deck}}}{E_{\text{conc}}}$$

(Eqn 4-4)

where

$\epsilon_{deck}$  = strain in the concrete deck, and

$E_{conc}$  = modulus of elasticity of concrete calculated as per ACI-08.

Optimized stresses are calculated by recalling the calculation of optimized moments in Chapter 3 and substituting Equation 3-39 into Equation 4-1. With algebraic rearrangement, the equation shown below gives the optimized Service II stress in the concrete deck shown in Equation 4-5.

$$\sigma_{deckOpt} = \frac{RF_{OTR} \cdot M_{servII}}{S_{deck}}$$

(Eqn 4-5)

Substituting the stress in Equation 4-5 into the strain equation, Equation 4-4, results in the following relation for optimized strain.

$$\epsilon_{deck} = \frac{RF_{OTR} \cdot \sigma_{deck}}{E_{conc}}$$

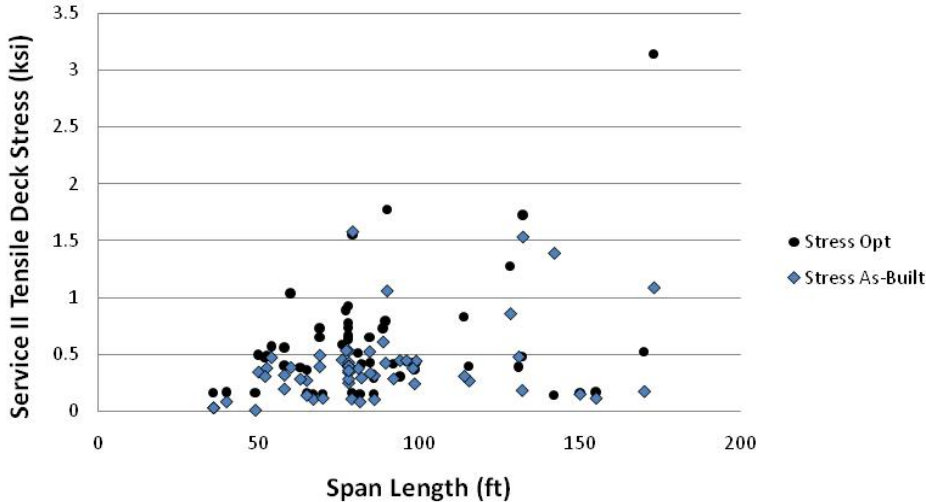
(Eqn 4-6)

### 4.3 Application of Procedure to BridgeTech Database Bridges

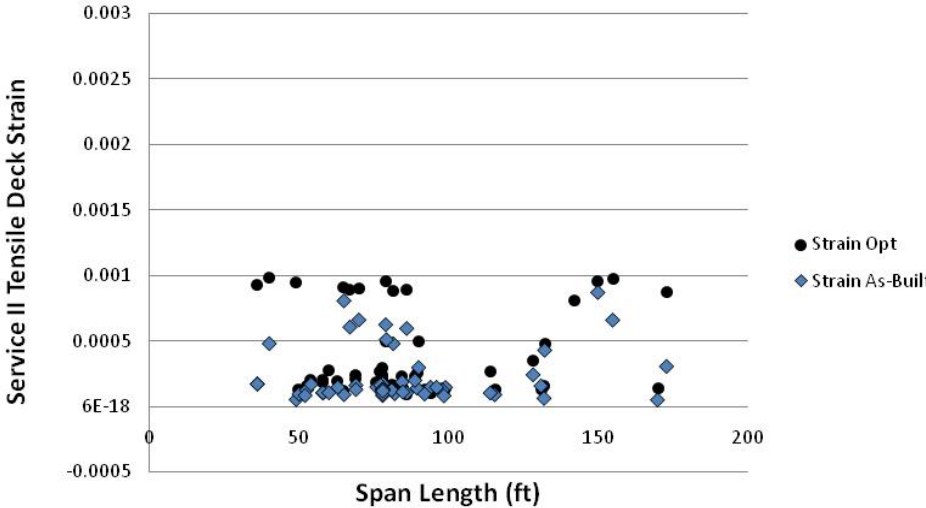
The procedure outlined in the previous section is applied to each continuous span bridge within the bridge suite. Figure 4-1 shows both the as-built and optimized stress in the concrete deck vs. the bridge span length.



Figure 4-2 shows the as-built and optimized concrete deck strains vs. the bridge span length. Figure 4-3 shows the as-built stress vs. the Service I deflections. Figure 4-4 shows the as-built strain vs. the Service I deflections.



**Figure 4-1 Tensile Stress in Concrete Deck vs. Span Length**



**Figure 4-2 Tensile Strain in Concrete Deck vs. Span Length**

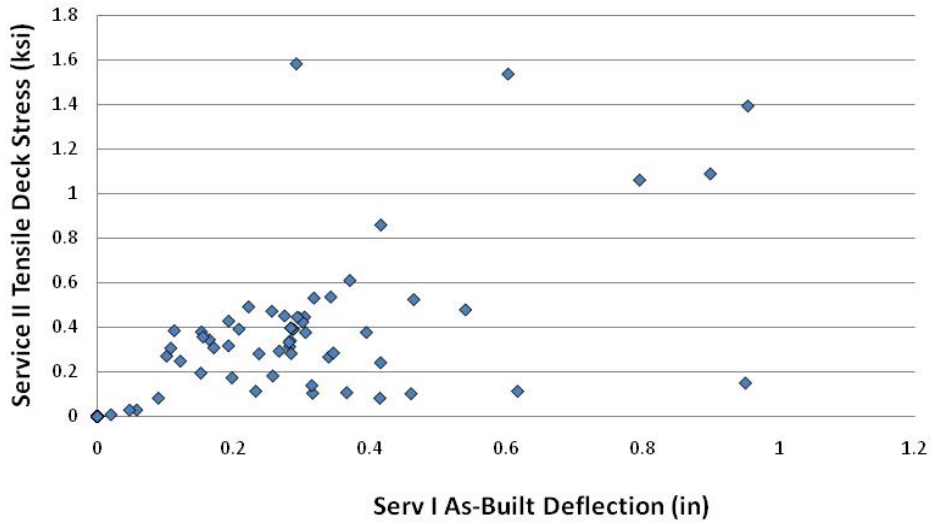


**Figure 4-3 Tensile Stress in Concrete Deck vs. Service I Deflection**

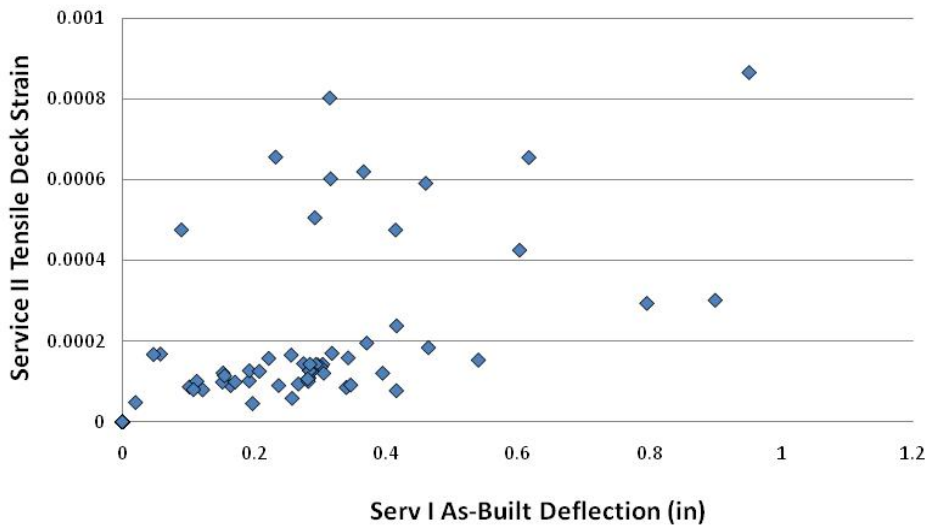


**Figure 4-4 Tensile Strain in Concrete Deck vs. Service I Deflection**

#### 4.4 Alternative Proposed Limit

From the figures, no significant correlation is observed between strain acting in the deck and Service I deflection or between strain acting in the deck and span length. Thus, from these plots, it is apparent that limiting deflections does not necessarily limit concrete deck stresses or strains. A new procedure is proposed below to directly control deck demands to control deformation-induced deck deterioration. As concrete is going to crack when the strain in the deck is equal to the concrete cracking strain, the following maximum strain limit is proposed in Equation 4-7.

$$\epsilon_{limite} = \frac{M_{SerII}}{E_{conc} \cdot S_{deck}}$$

(Eqn 4-7)

where

$S_{deck}$  = section modulus for top of concrete deck, short term composite,

$E_{conc}$  = modulus of elasticity of concrete, and

$M_{SerII}$  = peak negative moment at pier due to Service II loading.

While the formulation shown in Equation 4-7 is proposed, the final appropriate value of  $\epsilon_{lim}$  needs to be calibrated in future research.

## **4.5 Summary**

This chapter presents a proposed strain design limit for the pier regions of the concrete deck. The procedure was applied to the continuous span bridges of the bridgedatabase. The strains and stresses were compared to span length and Service I deflection. From these figures, no significant relation is observed between Service I deflections and tensile strain in the concrete deck. Since concrete cracks based on strain, the proposed limit to directly prevent deck deterioration presented is based on strain acting in the concrete deck.

## **Chapter 5 Summary, Conclusions and Future Work**

### **5.1 Summary**

Current AASHTO procedures offer serviceability criteria that are perceived to control user comfort and deformation-induced structural deterioration (deck cracking). However, studies show that current AASHTO serviceability criteria may be insufficient in controlling excess bridge vibrations (user comfort) and deck cracking (structural deterioration). The objectives of this research effort are to analyze the current AASHTO criteria and to develop alternative serviceability limits to prevent user discomfort and control flexural deck cracking. Two design criteria formulations are proposed. The first controls user comfort through controlling bridge vibrations. The second directly controls deformation-induced structural damage with a direct design limit on deck strains.

Chapter 2 details the development of the current AASHTO deflection criteria. Past research is referenced in order to demonstrate possible inadequacy of the current AASHTO deflection criteria in controlling user discomfort and structural deterioration. The movement in structural engineering to perform user comfort serviceability checks based on natural frequency is discussed. A detailed description of the bridge suite used in this research effort is also presented.

Chapter 3 derives a proposed user comfort formulation using a simple dynamic pluck test. From this pluck test a dynamic property of the bridge is obtained. The proposed criterion, while based on the dynamic property of the natural frequency, remains in deflection terms familiar to the typical bridge engineer. While the formulation is proposed, the final values for the design limits ( $X_{lim}$ ) require additional research for final calibration. The results of the optimization calculations are shown and discussed. The results indicate that the current AASHTO Service I criteria may be inadequate in controlling excess bridge vibrations and, therefore, user comfort. The results also indicate that the proposed user comfort formulation is a viable method warranting further development.

In Chapter 4, the behavior of the concrete deck slab is analyzed. The procedures used to determine the stress and strain are detailed. Finally, a proposed design criteria limit to control deformation-induced deck deterioration is presented.

## **5.2 Conclusions**

This section gives the conclusions for the current AASHTO Service I limits, the proposed design method for user comfort performance, and the proposed limit for concrete strain limit. It is important to note that these conclusions are based on the calibration to the Ontario Highway Bridge Design Code. It is also important to note that only the formulations of each

alternative serviceability limit are proposed by this research, not the actual design limit parameters ( $X_{lim}$  or  $\epsilon_{lim}$ ). Additional calibration is required to determine the final appropriate design limit parameters.

### **5.2.1 AASHTO Service I Deflection Limit Conclusions**

This section describes the conclusions associated with the current AASHTO Service I deflection limits. The adequacy for ensuring user comfort and adequacy for preventing deck deterioration are discussed.

The data in this study enables several conclusions regarding the adequacy of AASHTO Service I deflection limits in controlling user comfort. First, that for pedestrian bridges, the Service I deflection limits can be too liberal compared to other design codes. This suggests that it is possible that a heavy pedestrian use bridge satisfies the current AASHTO design code for user comfort, but performs in an unsatisfactory manner. Second, for vehicular bridges with no pedestrian traffic, the Service I deflection limits are overly conservative compared to other methods. These two conclusions, when considered together, point to a general inadequacy of the current AASHTO deflection limit. It should be noted that for heavy pedestrian bridges, the AASHTO code was not as prohibitive as previously thought; however, for vehicular bridges, the data does suggest that the Service I deflection limits are overly conservative.

By analyzing the data from Chapter 5, it is concluded that there is no notable relation between Service I deflection and strain in the concrete deck or between span length and strain in the concrete deck. This suggests that the AASHTO Service I deflection limits are an inadequate method for controlling flexural deck deterioration.

### 5.2.2 Alternative Proposed User Comfort Limit Based on $X_{lim}$ Conclusions

The ability to successfully relate  $X_{lim}$  to existing bridge codes based on natural frequency show that the proposed user comfort serviceability limit formulation is a viable method that warrants future research. The parameter  $X_{lim}$  for differing levels of pedestrian use needs additional calibration. The  $X_{lim}$  follows anticipated behavior of bridges and natural frequencies. The proposed limit successfully transforms a natural frequency based limit into a criterion with deflection terms familiar to bridge engineers. The proposed formulation of serviceability criteria to control excess bridge vibration is given in Equation 5-1:

$$\Delta_{fat} < \Delta_{max} = X_{lim} \cdot \frac{w \cdot L^4}{C_n^2 \cdot E \cdot I_x}$$

(Eqn 5-1)

where

- $\Delta_{Allow}$  = maximum allowable deflection,
- $\Delta_{fat}$  = deflection from the AASHTO fatigue truck loading,
- w = weight per unit length of bridge girder,



- L = span length,
- $I_b$  = transformed short term composite moment of inertia at midspan,
- E = modulus of elasticity of steel,
- $c_n^2$  = natural frequency correction factor for multi-span bridges, and
- $X_{lim}$  varies depending on level of pedestrian use (no pedestrian use, some pedestrian use, and heavy pedestrian use).

This research proposes that the expected daily load be used for controlling user comfort, as user comfort is a daily concern. Furthermore, a violation of user comfort by a rare maximum expected load is unlikely to cause a loss of structural integrity for the bridge structure. The lower occurrence frequency of these maximum expected loads is low enough to not warrant reducing bridge economy by designing for more conservative loadings. The fatigue truck load deflection is therefore proposed because it represents the expected daily load.

### **5.2.3 Alternative Proposed Concrete Strain Limit Conclusions**

To prevent deck deterioration requires more than simply limiting the strain in the concrete deck under Service level loads. There are many other factors that must be taken into account such as allowing for thermal expansion, taking into account beam deck interactions, proper drainage, etc. However, the proposed strain limit is an appropriate method to ensure that flexural deck deterioration does not occur directly from traffic loads. The proposed formulation for serviceability criteria to control deck cracking at

the piers is given by Equation 5-2. Note that  $\epsilon_{lim}$  requires additional research for full calibration.

$$\epsilon_{lim} = \frac{M_{SerII}}{E_{conc} S_{deck}}$$

(Eqn 5-2)

where

$S_{deck}$  = section modulus for top of concrete deck, short term composite,

$E_{conc}$  = modulus of elasticity of concrete,

$M_{SerII}$  = peak negative moment at pier due to Service II loading, and

$\epsilon_{lim}$  = limiting concrete tensile strain.

Deformation-induced structural deterioration is an maximum load occurrence. As such, the moment used to determine the direct flexural strain in the concrete deck is from the maximum expected serviceability load. As the Service II loading represents the largest expected load, the Service II moment is proposed for calculating flexural strain in the concrete deck.

### 5.3 Future Work

This section describes additional research that needs to be performed before both proposed serviceability criteria can be considered for adoption into the AASHTO code.

#### 5.3.1 Future Work for $X_{lim}$ User Comfort Method

In this work, the limiting X factor,  $X_{lim}$ , is correlated to the natural frequency vs. maximum deflection curve in the Ontario Bridge Code. However, it is unknown whether the OHBC is overly conservative, overly liberal, or neither. It is required that the  $X_{lim}$  method be fully calibrated. This calibration should include past work and possibly future work in finite element modeling, field testing of bridges, and further analysis. There are several bridges in the database used in this work that would be deemed suspect with the proposed criteria. These bridges would be good candidates for future study.

### **5.3.2 Future Work for Strain Limit**

As with the  $X_{lim}$  method for limiting excess bridge vibration, the strain limit,  $\epsilon_{lim}$ , designed to prevent flexural cracking in the concrete deck, requires additional research for full calibration. The limit needs to ensure an adequate factor of safety to ensure that cracking does not occur because of service level loads. The calibration process should include field tests, material testing, finite element analysis and further analysis in order to determine an adequate limiting strain.

## Works Cited

- '96 AUSTRALIAN BRIDGE Design Code (1996). SECTION SIX-CODE *Steel and Composite Construction*, AUSTRROADS, HAYMARKET, NSW, AUSTRALIA.
- AASHTO (2002), *Load Factor Design: Standard Specifications for Highway Bridges*, Seventeenth Edition, American Association of State Highway and Transportation Officials, Washington, D.C.
- AASHTO (2008), *Load Resistance and Factor Design: Bridge Design Specifications*, Third Edition, American Association of State Highway and Transportation Officials, Washington D.C.
- Allen, D.E., Murray, Thomas M., and Ungar, E.E. (1997), *Design Guide 11 Floor Vibrations Due to Human Activity*, American Institute of Steel Construction & Canadian Institute of Steel Construction, Chicago, IL.
- American Institute of Steel Construction. (2005), *Steel Construction Manual*, 13<sup>th</sup> Edition, Chicago, IL.
- Anderson, E. (2005), *Deflection Serviceability for Steel Girder Bridges*, Masters Thesis, University of Wyoming, Laramie, WY, December.
- Aramraks, T. (1975), *Highway Bridge Vibration Studies*, Joint Highway Research Project, Indiana State Highway Commission, Purdue University, West Lafayette, IN, February.
- Barker, M.G. and Barth, K.E. (2007), *Live Load Deflection Serviceability of HPS Composite Steel Girder Bridges*, 2007 World Steel Bridge Symposium Papers, New Orleans, LA, Dec.
- Barth, K., Bergman, A. and Roeder, C. (2002), *Improved Live Load Deflection Criteria for Steel Bridges*, Report to the National Cooperative Highway Research Program. University of Washington, Seattle, WA, May.

- Barth, K.E., Roeder, C.W., Christopher, R.A., and Wu, H. (2003), *Evaluation of Live Load Deflection Criteria for I-Shaped Steel Bridge Design Girders*, ASCE, Journal of Structural Engineering Special Publication – High Performance Materials in Bridges, 193 – 208.
- Barth, K., Bergman, A, and Roeder, C. (2004), *Effect of Live-Load Deflections on Steel Bridge Performance*, Journal of Bridge Engineering ASCE, University of Washington, Seattle, WA, May.
- Christopher, R.A. (2001), *Live Load Deflection Criteria for Steel I-Girder Bridges*, Masters Thesis. West Virginia University, Morgantown, WV, February.
- DeWolf, J.T., and Kou, J-W. (1997), *Vibrational Behavior of Continuous Span Highway Bridge-Influence Variables*, Journal of Structural Engineering, March.
- Fountain, R.S., and Thunman, C.E. (1987), *Deflection Criteria for Steel Highway Bridges*, Presented at National Engineering Conference, New Orleans, LA, April.
- Gandiaga, Lorehana (2009), *Serviceability Limits and Economical Bridge Design*, MS, Laramie WY, May
- Goodpasture, D.W., and Goodwin, W.A. (1971), *Final Report on the Evaluation of Bridge Vibration as Related to Bridge Deck Performance*, The Tennessee Department of Transportation, The University of Tennessee, Knoxville, TN.
- Nevels, J.B., and Hixon, D.C. (1973), *A Study to Determine the Causes of Bridge Deck Deterioration*, Final Report to the State of Oklahoma Department of Highways. Oklahoma City, OK.
- Ontario Highway Bridge Design Code*, Second Edition (1983), Ontario Ministry of Transportation and Communications Highway Engineering Division, Toronto, Ontario.
- Walker, W.H., and Wright, R.N. (1971), *Criteria for the Deflection of Steel Bridges*, Bulletin for the American Iron and Steel Institute, November.

Wu, Haiyong (2003). *Influence of Live-Load Deflections on Superstructure Performance of Slab on Steel Stringer Bridges*. Doctoral dissertation, College of Engineering and Mineral Resources at the University of West Virginia, Morgantown, WV.